universität wien

DIPLOMARBEIT

Titel der Diplomarbeit

Generation and characterization of the postfusion structure of the major surface protein E of tick-borne encephalitis virus

Verfasserin

Andrea Bernhart

angestrebter akademischer Grad

Magistra der Naturwissenschaften (Mag.rer.nat.)

Wien, 2012

Studienkennzahl lt. Studienblatt:		A 490
Studienrichtung lt. Studienblatt:		Diplomstudium Molekulare Biologie
Betreuerin / Betreuer:		Ass.-Prof. Priv.-Doz. Dr. Karin Stiasny

Ich möchte mich bedanken….

….bei Prof. Franz Xaver Heinz der mir diese Diplomarbeit am Department für Virologie ermöglicht hat

….bei Ass.-Prof. Priv.-Doz. Dr. Karin Stiasny für die wissenschaftliche Betreuung meiner Diplomarbeit

….bei meinen Kollegen, die mir immer mit Rat zur Seite standen und den Arbeitstag mit Humor bereicherten

….bei meinen Freunden für ihre geduldigen offenen Ohren

….bei meiner Familie, allen die ich so nennen darf und Tom für ihre Liebe und Unterstützung

Table of contents

1 Abstract

Flaviviruses enter cells by receptor-mediated endocytosis and fuse their membrane with that of the endosome. Fusion is triggered by the acidic pH of this compartment and mediated by dramatic structural changes of the viral envelope protein E. Exposure to low pH induces an oligomeric rearrangement of E in which the subunits of the native E homodimers dissociate and the monomeric subunits then reassociate into more stable homotrimers. Crystal structures of truncated E proteins in their pre- and postfusion conformation lack the so called 'stem' region (located between the ectodomain and the membrane anchor) which is hypothesized to be critically required for fusion. Fusion models predict that during the dimer-trimer-transition the stem „zippers" along the trimer and that these interactions are essential for bringing the host and viral membrane into close proximity. This diploma thesis focused on the generation and characterization of soluble forms of E (sE) in their postfusion conformation with the stem (or parts thereof) for further analyses including the determination of the three-dimensional structures by X-ray crystallography. Knowledge of such structures would shed novel light on the precise role of the stem for membrane fusion. For this purpose, two different sE proteins of tick-borne encephalitis (TBE) virus were expressed using stably transfected Drosophila cell lines TBE sEH1H2, containing the whole stem region, and TBE sEH1, containing only parts of the stem. sEH1 was expressed with a strep tag which was also used for its purification. This protein was secreted predominantly as a dimer and after purification and removal of the tag the protein was converted into trimers by exposure to low pH in the presence of liposomes. The sEH1H2 protein, in contrast, was already found to be in its trimeric postfusion form in the cell culture supernatant. Due to the increased hydrophobicity of sEH1H2 compared to sEH1, detergents were required for purification experiments. Although further optimization will be necessary to obtain large amounts of highly purified sEH1H2 trimers for crystallization, preliminary studies with monoclonal antibodies were possible and allowed the identification of important interactions of the stem-region with other parts of E in the postfusion trimer.

Zusammenfassung

Flaviviren dringen mittels Rezeptor-vermittelter Endozytose in Zellen ein und fusionieren ihre Membran mit der des Endosoms. Fusion wird durch dramatische strukturelle Änderungen des virale Hüllproteins E (“envelope“) vermittelt, die der saure pH des Endosoms induziert. Eine Reorganisation der Oligomere des E-Proteins ist die Folge, bei der die Untereinheiten des E-Proteins in Monomere dissoziieren und sich aus diesen stabilere Trimere formen. Den bisher bekannten Kristallstrukturen der E-Proteine vor und nach der Fusion (Prä- und Post-Fusions-Struktur) fehlt die so genannte "Stamm" Region (zwischen der Ektodomäne und dem Membran-Anker) und die Transmembranregion. Der Stamm ist vermutlich für die Fusion essentiell. In Fusionsmodellen wird vorgeschlagen, dass während der Dimer-Trimer-Umlagerung der Stamm sich reißverschlussartig am Trimer anlagert (“zippering“) und dass diese Wechselwirkungen für die räumliche Annäherung von der viralen Membran an die Membran der Wirtszelle wesentlich sind.

Diese Diplomarbeit konzentrierte sich auf die Herstellung und Charakterisierung von löslichen Formen des E-Proteins (sE) in seiner Post-Fusions-Konformation, die den Stamm oder Teilen davon enthält. Diese Proteine können für weitere Analysen verwendet werden, vor allem für die Bestimmung der dreidimensionalen Strukturen mit Hilfe der Röntgenkristallographie. Die Kenntnis solcher Strukturen kann zu einem besseren Verständnis für die Rolle des Stamms in der Membranfusion führen. Zu diesem Zweck wurden zwei unterschiedliche sE Proteine des Frühsommer-Meningoenzephalitis (FSME)-Virus in stabil transfizierten Drosophila-Zelllinien exprimiert: TBE sEH1H2, das die gesamte Stamm-Region enthält und TBE sEH1, das nur Teile des Stamms enthält. sEH1 wurde mit einem Strep-Tag hergestellt, der auch für die Reinigung des Proteins verwendet wurde. sEH1 wurde überwiegend als Dimeres sezerniert und, nach der Aufreinigung und der Entfernung des Tags, in Gegenwart von Liposomen bei saurem pH trimerisiert. Im Gegensatz dazu lag sEH1H2 bereits als Trimeres im Zellkulturüberstand vor. Aufgrund der erhöhten Hydrophobizität von sEH1H2 im Vergleich zu sEH1 waren Detergenzien für die Aufreinigung erforderlich. Obwohl weitere Optimierungen notwendig sind, um große Mengen an hochreinen sEH1H2 Trimeren zur Kristallisierung herzustellen, erlaubten

vorläufige Untersuchungen mit monoklonalen Antikörpern die Identifizierung von wichtigen Wechselwirkungen der Stamm-Region mit anderen Teilen des E-Proteins im Post-Fusions-Trimer.

2 Introduction

2.1 General introduction

2.1.1 Family Flaviviridae, genus Flavivirus

The family Flaviviridae comprises three genera: Flavivirus (Latin “flavus” meaning yellow) Pestivirus (Latin “pestis” meaning plague) and Hepacivirus (“hepar” translated from Greek as liver). All three genera show similarities in replication, morphology and composition of the viral genome (Lindenbach B.D. Thiel H-J., 2007).

Flavivirus is the largest of the three genera and contains more than 70 distinct viruses. This genus can be subdivided into serocomplexes and phylogenetical groups (Kuno et al., 1998) (Figure 1).

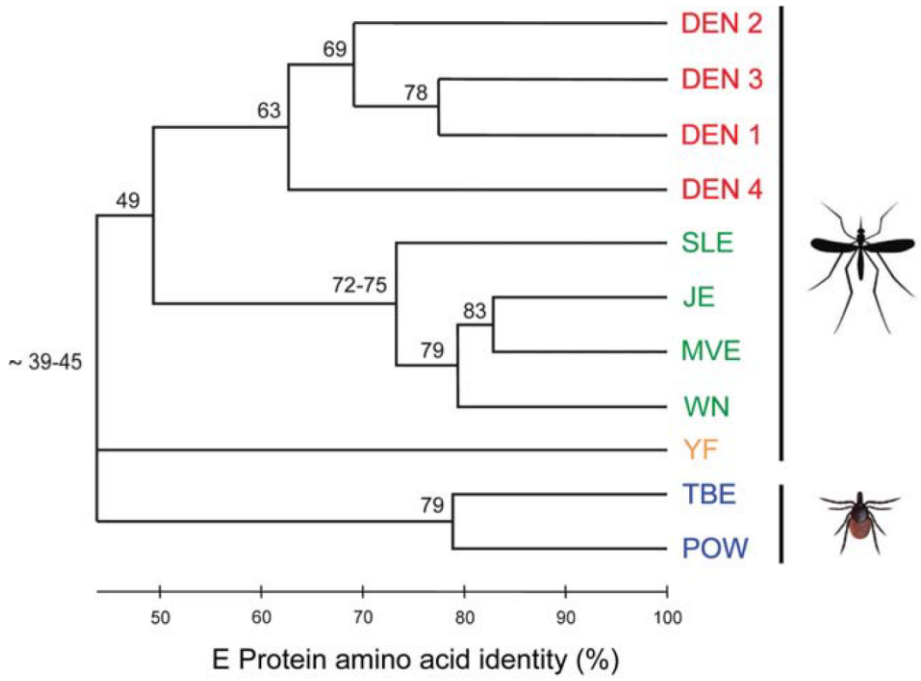

Figure 1 Flavivirus classification. Relationships are depicted according to the identity of the amino acid sequence of the envelope protein (E protein). Four serocomplexes are shown: in *red*: DENV (dengue virus) serocomplex, *green*: JEV (japanese encephalitis virus) serocomplex, *yellow*: YFV (yellow fever virus) serocomplex and in *blue*: TBEV (tick-borne encephalitis virus) serocomplex. On the right side the corresponding transmission vector is shown. (Figure adapted from (Stiasny et al., 2006)

The majority of flaviviruses is arthropod-borne either by ticks or mosquitoes, but for some flaviviruses the vector is unknown (Kuno et al., 1998). Tick-borne encephalitis virus (TBEV) is transmitted by ticks, while other important human pathogens, like yellow fever virus (YFV), dengue viruses (DENV 1-4), Japanese encephalitis virus (JEV) and West Nile virus (WNV) are transmitted by mosquitoes (Gubler, 2007) (Figure 1).

2.1.2 Transmission, epidemiology

TBEV is transmitted by infected ticks that pass the virus on in their saliva. In addition, milk-borne TBE is possible after consumption of unpasteurized milk or milk-products from viraemic animals, especially goats (Holzmann et al., 2009; Lindquist and Vapalahti, 2008).

TBEV is endemic in many European countries, Asian parts of Russia, northern Japan and northern China. The habitat of ticks is restricted by suitable temperatures (6-25 C°) and a humidity higher than 85% (Lindquist and Vapalahti, 2008). Three subtypes of TBEV are described: the European, the Sibirian and the Far Eastern subtype (Ecker et al., 1999). The European subtype is transmitted by *Ixodes ricinus*, while the other two subtypes use *Ixodes persulcatus* as a vector (Lindquist and Vapalahti, 2008). Within a subtype a low variation in the amino acid sequence of the E protein of maximal 2.2% was found; between the three different subtypes the maximum of variation was 5.6% (Ecker et al., 1999).

2.2 Morphology and Organization

2.2.1 Genome

The genome of flaviviruses is organized in a positive single stranded RNA of approximately 11 kb (Figure 2). A single open reading frame (ORF) encodes seven non-structural (NS1, NS2a, NS2b, NS3, NS4a, NS4b, NS5) and three structural proteins (capsid C, envelope E and precursor of membrane protein prM/M). The ORF is flanked by 3’ and 5’ non coding (NCR) regions that are important for replication.

The 5’ end is capped by $m^7GpppAmpN_2$ (Lindenbach B.D. Thiel H-J., 2007). The ORF is translated into one large polyprotein, that is proteolytically processed into the viral proteins (Lindenbach B.D. Thiel H-J., 2007) (Figure 3).

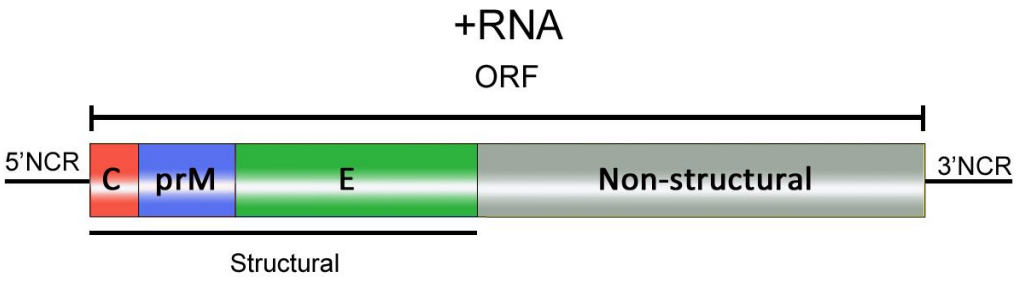

Figure 2 Schematic representation of the flavivirus RNA genome (not to scale). The open reading frame (ORF) codes for structural and non-structural proteins. Non coding regions at the 3’ and 5’ ends flank the ORF.

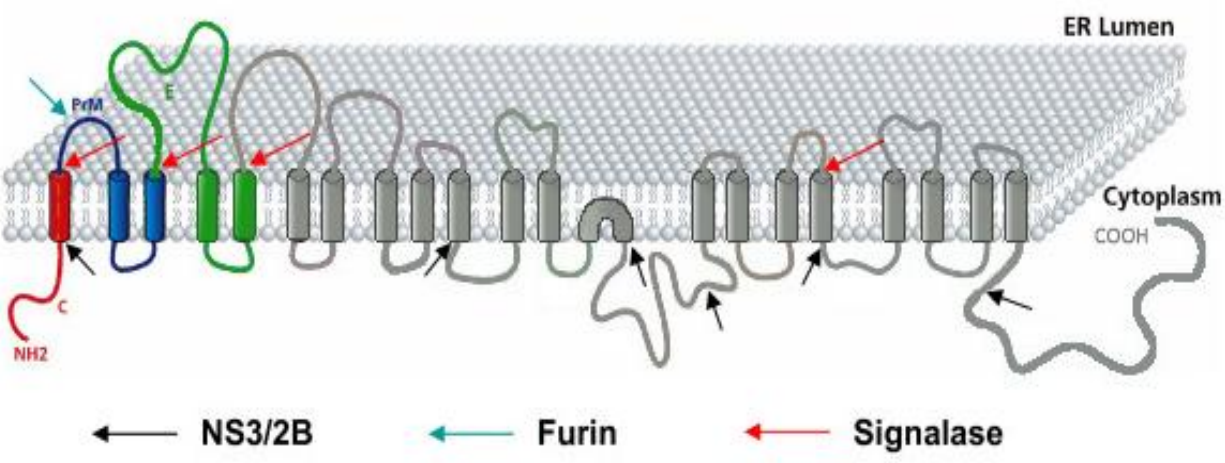

Figure 3 Schematic representation of the endoplasmic membrane topology of the flavivirus polyprotein. In red protein C, in blue glycoprotein prM, in green envelope glycoprotein E and in grey the non-structural proteins. (Figure adapted from (Umareddy et al., 2007))

2.2.2 Structural organization of flaviviruses

Flaviviruses are enveloped viruses with an icosahedral organized envelope of approximately 500 Å in diameter (Mukhopadhyay et al., 2005). Three proteins build the viral particle: two membrane associated proteins (prM/M, E) and the capsid

protein (C) that builds together with the viral genome the nucleocapsid. Virions are assembled as immature particles, containing prM/E heterodimers that form trimeric spikes (Zhang et al., 2003b). During maturation the pr-peptide is proteolytically cleaved leaving the M protein anchored in the lipid bilayer and conformational changes take place on the viral surface (Lindenbach B.D. Thiel H-J., 2007; Mukhopadhyay et al., 2005).

The mature virion has a smooth, tightly packed surface with the E protein in a dimeric conformation (Kuhn et al., 2002; Mukhopadhyay et al., 2003; Mukhopadhyay et al., 2005) (Figure 4).

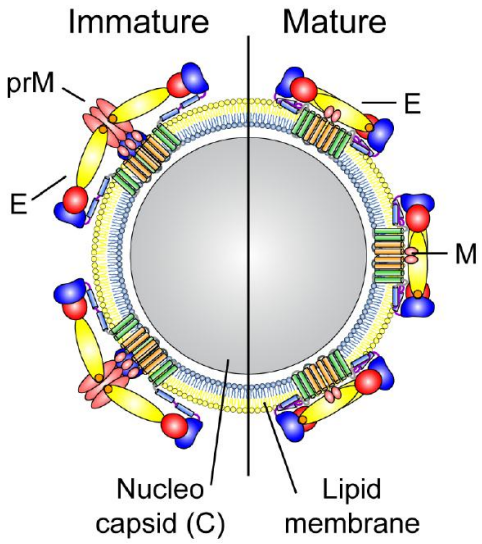

Figure 4 Flavivirus particles. Left: immature particles with heterodimeric prM/E complexes. Right: mature particles with E homodimers. (Figure adapted from (Stiasny and Heinz, 2006))

2.2.3 Life cycle

The viral life cycle (Figure 5) starts with the attachment of the virion to the cell by receptor binding of the E protein. This is followed by receptor-mediated clathrin-dependent endocytosis (van der Schaar et al., 2008). Due to the acidic pH (< 6.6) in the endosome, structural alterations are induced in E, leading to fusion of the viral membrane with the endosomal membrane. Subsequently, the viral nucleocapsid is released into the cytoplasm. After uncoating the positive stranded RNA genome is replicated and translated. Virus assembly occurs in the endoplasmic reticulum (ER), leading to the formation of non-infectious immature virions. In this state, prM is

associated with E in a heterodimeric complex to prevent E-mediated fusion (Heinz et al., 1994). During exocytosis prM is cleaved by furin or a furin-like protease in the trans-Golgi network (TGN) before virions are released from the cell (Mukhopadhyay et al., 2005). The neutral pH in the extracellular space causes the pr-part to detach from the viral particle (Yu et al., 2008) resulting in mature infectious particles. Together with infectious virus particles slowly-sedimenting hemagglutinin (SHA) particles are released from infected cells (Heinz and Kunz, 1977). SHA particles lack the nucleocapsid and are therefore noninfectious (Lindenbach B.D. Thiel H-J., 2007).

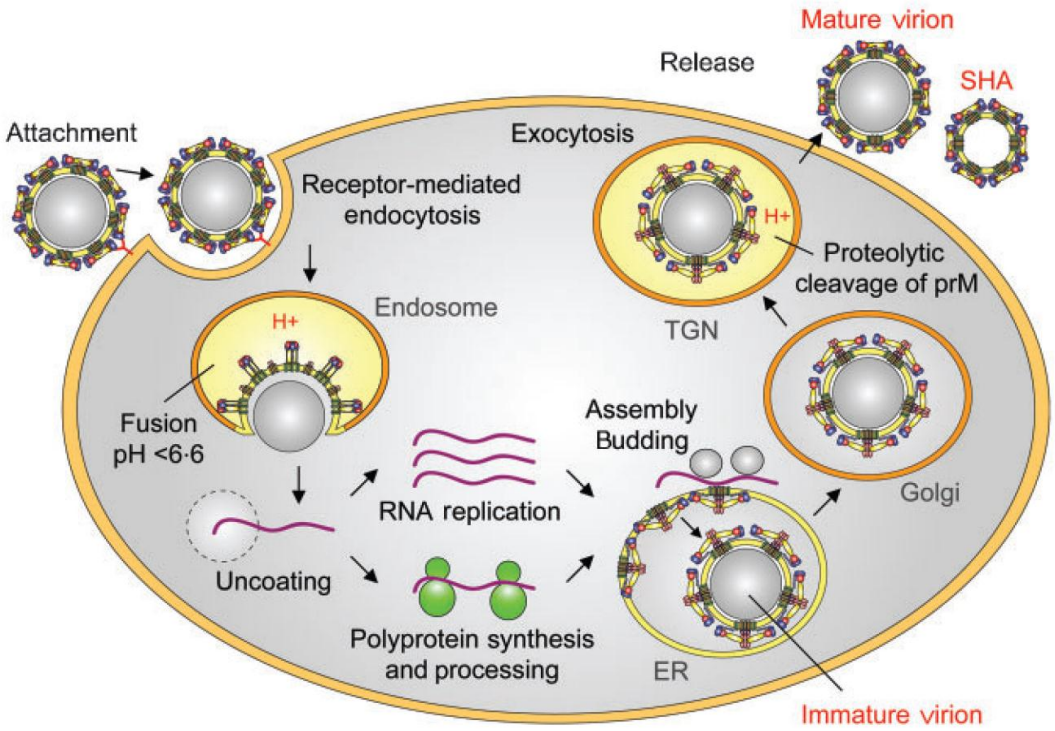

Figure 5 Schematic representation of the flavivirus life cycle.

ER: endoplasmic reticulum

TGN: trans-Golgi Network

SHA: Slowly-sedimenting hemagglutinin

(Figure adapted from (Stiasny and Heinz, 2006))

2.2.4 Structural proteins

2.2.4.1 C protein

The C protein (11 kd) is highly basic and largely α-helical with internal hydrophobic regions (Mukhopadhyay et al., 2005). Due to the positive charge of the protein, it associates with the negatively charged viral genome (Lindenbach B.D. Thiel H-J., 2007; Mukhopadhyay et al., 2005). The hydrophobic regions interact with the viral membrane (Lindenbach B.D. Thiel H-J., 2007; Mukhopadhyay et al., 2005).

2.2.4.2 Membrane glycoprotein prM / M

The main function of prM is to assist the E protein in proper folding and to prevent the conversion of E into its fusogenic state in acidic compartments of the secretory pathway (Lindenbach B.D. Thiel H-J., 2007; Lorenz et al., 2002).

The membrane protein is expressed as prM, the precursor of the M protein. The prM protein is about 26 kd and its N-terminal region contains three N-linked glycosylation sites and six conserved cystein residues that build three disulphide bridges (Chambers et al., 1990; Nowak et al., 1989).

The prM protein is integrated into the ER membrane by two trans-membrane spanning helices (Figure 3). In immature viruses, it forms heterodimers with the E protein. During exocytosis of these particles, prM is cleaved by furin. Upon secretion into the neutral pH of the extracellular space the pr-part of prM dissociates (Li et al., 2008; Stiasny et al., 1996; Yu et al., 2009), M (about 8kd) remains associated with the viral particles and E forms homodimers (Lindenbach B.D. Thiel H-J., 2007; Mukhopadhyay et al., 2005).

2.2.4.3 Envelope glycoprotein E

The E protein mediates important functions during cell entry, i.e. receptor binding and membrane fusion after virus uptake by endocytosis (Kaufmann and Rossmann, 2011; Kielian, 2006; Lindenbach B.D. Thiel H-J., 2007; Stiasny and Heinz, 2006).

After the E protein is cleaved by a host signalase it is anchored in the membrane by two transmembrane domains (Figure 3). Twelve cysteines form disulphide bonds and E can be glycosylated and in most flavivirus species E contains an N-type linked oligosaccharide (Lindenbach B.D. Thiel H-J., 2007).

The size of the E protein is approximately 53kd. The crystal structure of the soluble ectodomain of the E protein (sE; residues 1-400) has been solved for several flaviviruses (Luca et al., 2011; Modis et al., 2003; Modis et al., 2005; Nybakken et al., 2006; Rey et al., 1995; Zhang et al., 2004). The crystallized ectodomain is connected to the double membrane anchor via the “stem” region that contains two amphipathic helices, helix 1 and helix 2 (Zhang et al., 2003a). The ectodomain possesses three distinct structurally defined domains: The central domain I (DI) at the N-terminus, the dimerization region domain II (DII) and the Ig-like domain III (DIII) at the C-terminus. In all three domains, ß-sheets are predominant and all domains are joined by flexible hinges (Rey et al., 1995) (Figure 6). The tip of domain II contains a hydrophobic, conserved sequence element (fusion peptide), that is important for membrane fusion (Allison et al., 2001).

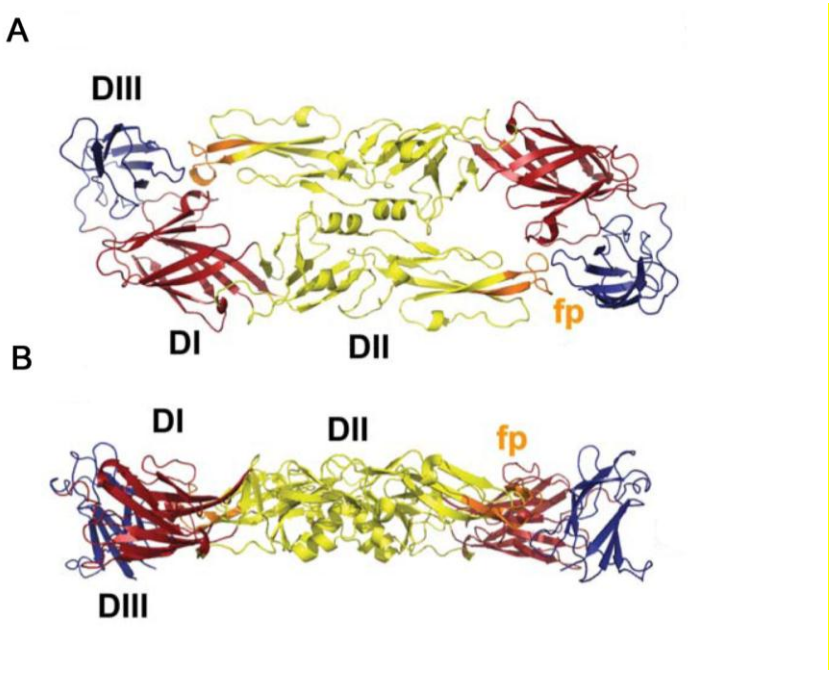

Figure 6 Ribbon diagrams of the sE dimer (A) top view and (B) side view. Color code: DI in red, DII in yellow, DIII in blue, fusion peptide (fp) in orange. (Figure adapted from (Stiasny and Heinz, 2006))

2.2.4.4 The stem anchor region of E

The region connecting the E protein ectodomain to the double trans-membrane anchor, the so called “stem” is about 50 amino acids long (Stiasny et al., 1996; Zhang et al., 2003a). It includes two amphipathic helices, helix 1 and helix 2, flanking a central conserved sequence (CS) element (Zhang et al., 2003a) (Figure 7). The stem region has increasing hydrophobicity towards the C-terminus (Schmidt et al., 2010b).

Cryo-EM has shown that the stem helices are half buried in the outer leaflet of the viral membrane, underneath the ectodomain (Zhang et al., 2003a).

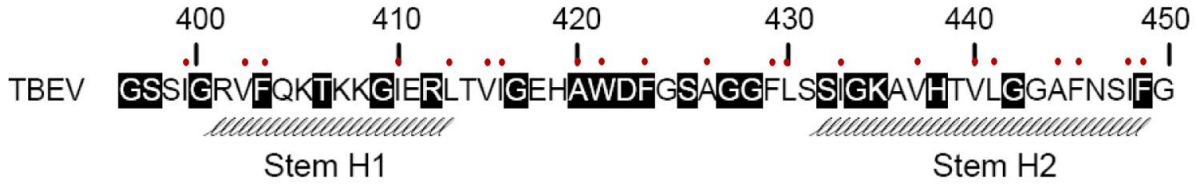

Figure 7 Carboxy terminal amino acid sequence of TBEV. Highlighted in black are amino acids conserved among flaviviruses. Red dots indicate hydrophobic amino acids. The two stem helices are depicted underneath the sequence according to helix prediction from Stiasny et al. (figure adapted from (Stiasny et al., 1996)).

2.2.4.5 Structural organization of flavivirus particles

Cryo-EM studies and image reconstruction of mature flaviviruses particles revealed an icosahedral organization of the virus surface. 180 E proteins form a herringbone-like lattice of 30 rafts of 3 E protein homodimers (Kuhn et al., 2002; Mukhopadhyay et al., 2003) (highlighted in figure 8B). Mature viruses have a smooth, spikeless envelope of 50nm diameter.

Immature virions are slightly bigger, with a diameter of about 60 nm (Lindenbach B.D. Thiel H-J., 2007) and contain 60 spikes on their surface, each composed of three prM/E heterodimers (Zhang et al., 2003b) (Figure 8A).

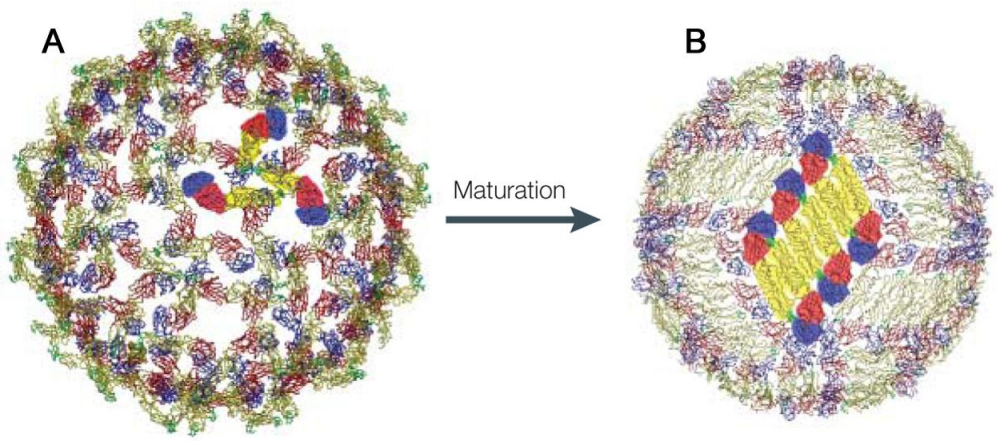

Figure 8 Pseudo-atomic structures of the surface of immature (A) and mature (B) flavivirus virions based on cryo-EM reconstructions.(B) A raft of three dimers is highlighted. Color code: DI in red, DII in yellow and DIII in blue, fusion peptides in green. (Figure from (Mukhopadhyay et al., 2005))

2.3 Membrane Fusion

2.3.1 Viral fusion proteins

In the life cycle of an enveloped virus, membrane fusion with its target cell is a crucial event. This process has to be tightly regulated to occur at the right time and place (Harrison, 2008). Membrane fusion is mediated by viral fusion proteins (glycoproteins) that are present in a metastable conformation on the surface of mature virions and undergo triggered conformational changes necessary for fusion (Harrison, 2005; Schibli and Weissenhorn, 2004). Possible triggers are (i) receptor binding, (ii) exposure to a low pH or (iii) both (White et al., 2008).

Three structural classes of viral fusion proteins can be distinguished (Weissenhorn et al., 2007; White et al., 2008):

Class I: Members of class I, such as orthomyxo-, paramyxo-, retro-, corona- and filoviruses share similarities with cellular SNARE fusion proteins (Skehel and Wiley, 1998). The structure of class I is characterized by homotrimers with a central α-helical coiled-coil (Kielian and Rey, 2006). The fusion peptide of class I is located at or near the N-terminus of the fusion subunit (White et al., 2008). For class I fusion

proteins processing of the fusion protein itself is typically required to be fusion competent (Harrison, 2005; Skehel and Wiley, 2000).

Class II proteins of flavi- (E) and alphaviruses (E1) possess internal fusion peptide loops between two ß-sheets. E and E1 are oriented parallel to the viral membrane and build an icosahedral oligomeric network (Harrison, 2008; Kuhn et al., 2002; White et al., 2008; Zhang et al., 2003a).

Class III fusion proteins are found in rhabdo-, herpes- and baculoviruses (Backovic and Jardetzky, 2009). They share similarities with both, class I and class II fusion proteins (Weissenhorn et al., 2007). Class III fusion proteins possess an internal fusion loop that is not as conserved as in class I and class II fusion proteins (Backovic and Jardetzky, 2009). The fusion loop of class III fusion proteins is located in domain I.

Despite the structural unrelatedness, all fusion proteins undergo conformational changes that mediate fusion involving the exposure of the fusion peptide that interacts with the target membrane and the formation of a hairpin-like postfusion structure with the fusion peptide and the transmembrane anchors juxtaposed at the same end of the protein rod (Kielian and Rey, 2006; Stiasny and Heinz, 2006; Weissenhorn et al., 2007).

2.3.2 Class II viral fusion protein E

The structure of the ectodomain of the truncated envelope glycoprotein E has been resolved in its pre- and the postfusion conformation for several flaviviruses (Bressanelli et al., 2004; Kanai et al., 2006; Luca et al., 2011; Modis et al., 2003; Modis et al., 2004; Modis et al., 2005; Nayak et al., 2009; Nybakken et al., 2006; Rey et al., 1995; Zhang et al., 2004).

As outlined in “2.2.4.3 Envelope glycoprotein E” the ectodomain possesses three domains (DI, DII and DIII).

In the metastable, mature prefusion conformation, the dimer has a head-to-tail arrangement and is orientated parallel to the viral membrane (Rey et al., 1995). The fusion peptide at the tip of DII is buried in a hydrophobic pocket provided by DI and

DIII of the partner subunit. An oligosaccharide additionally covers the fusion peptide (Rey et al., 1995) (Figure 9 A, B).

In the postfusion conformation, the E protein forms trimers that are orientated perpendicular to the membrane and the domains are arranged head-to-head (Bressanelli et al., 2004; Modis et al., 2004; Nayak et al., 2009) (Figure 9 C, D). DII is rotated 19° around the DI/ DII hinge and DIII is relocated to the side of DI, 33 Å from its prefusion position (Bressanelli et al., 2004; Modis et al., 2004) (Figure 10). This enables the formation of a hairpin-like structure in which the fusion peptide is juxtaposed to the membrane anchors (Bressanelli et al., 2004). Although the domains change their position towards each other, their original folds remain (Stiasny and Heinz 2006).

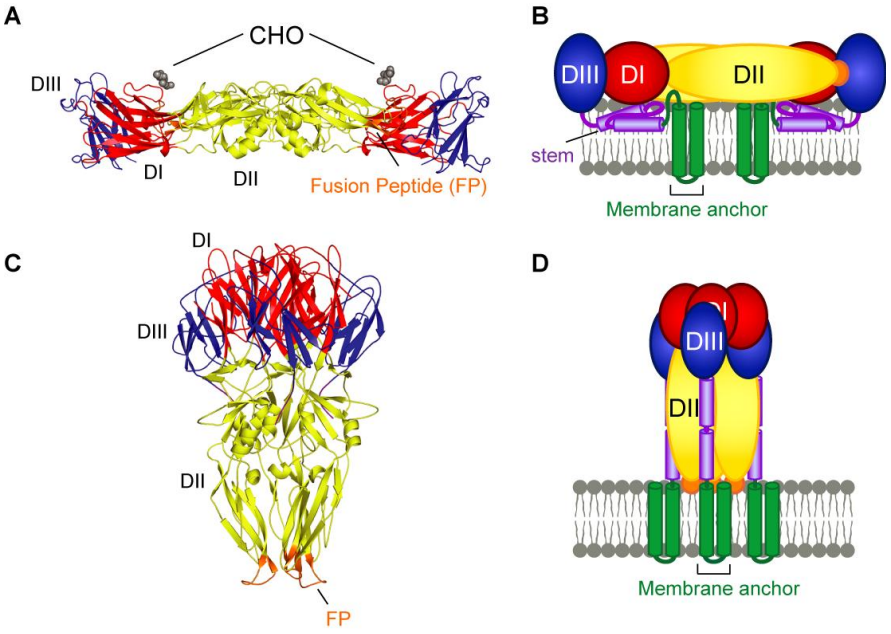

Figure 9 Ribbon diagrams and schematics of the TBEV E protein in its pre- and postfusion state. (A, B) The dimeric prefusion conformation. (C, D) The trimeric postfusion conformation. The position of the stem anchor region is based on the study of (Bressanelli et al., 2004). Color code: DI in red, DII in yellow and DIII in blue, fusion peptides in orange, stem region in purple, transmembrane region in green. (Figure adapted from (Stiasny and Heinz, 2006))

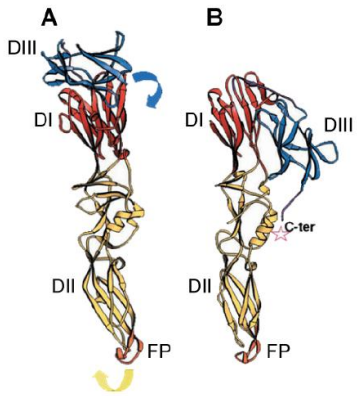

Figure 10 Ribbon diagrams of monomeric subunits before (A) and after (B) fusion. Color code: DI in red, DII in yellow and DIII in dark blue, fusion peptides in orange. Arrows indicate the direction of rotation. C-terminus is depicted as asterisk. (Figure from (Bressanelli et al., 2004)).

2.3.2.1 Flavivirus fusion mechanism

Fusion of flaviviruses is a fast and efficient process (Stiasny and Heinz, 2006). A fusion model was developed based on the X-ray structures of the pre- and postfusion E proteins together with biochemical studies (Figure 11 A-E). Flaviviruses enter the host cell by receptor-mediated endocytosis. In the endosomal compartment, the virus is exposed to acidic pH that triggers the E protein dimers to dissociate (Stiasny et al., 1996). In this monomeric state the fusion peptides are exposed and are able to insert into the target membrane (Stiasny et al., 2002). It has been speculated that the extension of the stem facilitates the insertion of the fusion peptide into the target membrane (Kaufmann et al., 2009) (Figure 11 B).

At this stage the two lipid bilayers are held together by the E protein; on one side anchored in the viral membrane by the transmembrane domain, on the other side attached to the target membrane via the fusion peptides. As the conformational change proceeds - involving the relocation of DIII and trimerization - the two membranes are drawn together (Figure 11 C-E). The protonation of amino acid residues at the domain I / domain III interface has been shown to be essential for the destabilization of this region (Fritz et al., 2008), which is necessary for the release of the fusion peptide from its buried position in the dimer as well as for the relocation of DIII. Fusion is then believed to continue by “zippering” of the stem along the body of

the trimer (Figure 11 C, D), thus forcing the formation of a hemifusion intermediate with only the outer leaflets fused (Figure 11 D) (Schmidt et al., 2010b). The final step would be the juxtaposition of the membrane anchor and the fusion peptides (postfusion structure) for the formation of a fusion pore (Figure 11 E).

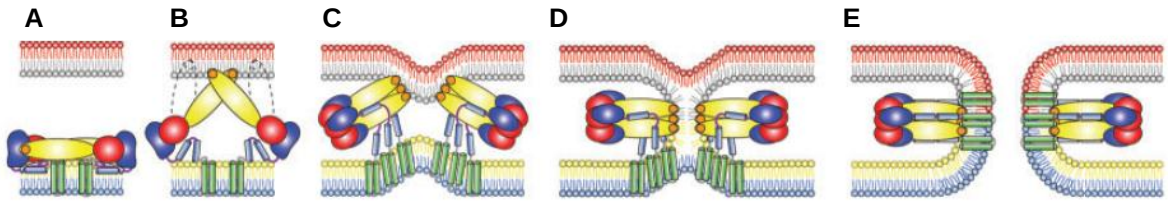

Figure 11 Proposed fusion process for class II. The color code referring to the domains: DI in red, DII in yellow, DIII in blue, fusion peptide in orange, stem region in blue, transmembrane region in green. Mechanism as explained in the text (Figure from (Stiasny and Heinz, 2006))

2.3.2.2 The stem and flavivirus membrane fusion

The structure of sE in its postfusion conformation has been elucidated (Bressanelli et al., 2004; Modis et al., 2004; Nayak et al., 2009), but the arrangement of the stem region is not known. In a modeling analysis, stem helix 1 could be fitted into the groove of two adjoining DII of the sE postfusion structure (Bressanelli et al., 2004), but not helix 2 (Figure 12). It is therefore possible that the postfusion conformation of the E protein, including the stem, could be different from the stem-less truncated version (Bressanelli et al., 2004).

In the fusion process, the stem is thought to play an important role, providing part of the energy for fusion by zippering. Schmidt et al., 2010 have shown that externally applied DENV E protein stem peptides inhibited viral infectivity (Schmidt et al., 2010a) and that such peptides could cross-inhibit different dengue viruses, but not other flaviviruses (Schmidt et al., 2010b).

Additionally, a mutagenesis study has revealed that a specific interaction between a hydrophobic pocket in DII and helix 1 of the stem is necessary in late stages of the fusion process and contributes to the stability of the postfusion trimer (Pangerl et al., 2011). Consistent with this finding, it was shown that the thermostability of full-length trimers was higher than that of truncated sE

trimers (Stiasny et al., 2005).

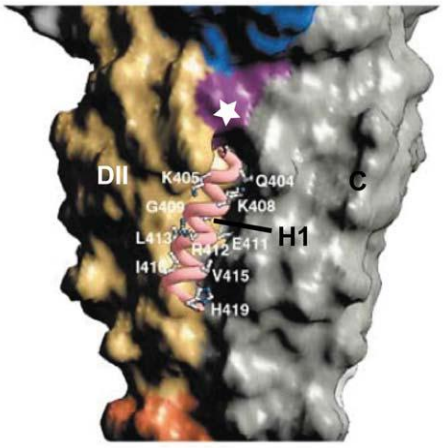

Figure 12 Surface representation of part of the sE trimer with the stem helix 1 (pink) modeled into the grooves formed by domain IIs. The crystallized c-terminus is labelled with a white star. (Figure adapted from (Bressanelli et al., 2004))

2.3.2.3 Comparison of the E protein with the alphavirus fusion protein E1

Despite the absence of sequence conservation, the structures of the alphaviral and flaviviral ectodomains of the fusion proteins are homologous in their secondary and tertiary structures (Lescar et al., 2001) (Figure 13). Both viruses share the overall organisation of the fusion protein into three domains (DI, DII, DIII), including the position of the fusion peptide at the tip of DII (Bressanelli et al., 2004; Lescar et al., 2001).

Regardless of several shared features of the class II fusion proteins of alphaviruses and flaviviruses, there are some differences in the fusion machinery:

On the surface of flaviviruses the E protein is present in a herring-bone-like pattern of rafts of three homodimers (Kuhn et al., 2002; Mukhopadhyay et al., 2003; Mukhopadhyay et al., 2005; Zhang et al., 2004). In contrast, 80 trimeric spikes of E1/ E2 heterodimers cover the surface of mature alphaviruses in a T=4 symmetry (Mukhopadhyay et al., 2006; Strauss et al., 2002; von Bonsdorff and Harrison, 1975).

The E protein of flaviviruses is responsible for both entry functions, binding to the cell receptor and fusion, whereas E1 mediates fusion and E2 is the receptor-binding protein (Mukhopadhyay et al., 2006).

The ~54 amino acids long stem region of TBEV has a conserved secondary structure (Stiasny et al., 1996; Zhang et al., 2003a). In alphaviruses the stem is less ordered and has a length of ~30 amino acids (Liao and Kielian, 2006a; Liao and Kielian, 2006b). It was shown that a minimal stem length of at least 9 amino acids was required for fusion (Liao and Kielian, 2006a).

The E protein of flaviviruses is anchored with a double transmembrane region in the viral membrane (Zhang et al., 2003a). In contrast, the alphavirus glycoprotein E1 has a single transmembrane domain (Jose et al., 2009; Strauss et al., 2002).

In the flavivirus postfusion trimer the fusion peptides interact with each other ("closed conformation"), whereas in the E1 postfusion trimer the three fusion peptides are about 45 Å apart ("open conformation") (Bressanelli et al., 2004; Gibbons et al., 2004a) (Figure 13 B, D).

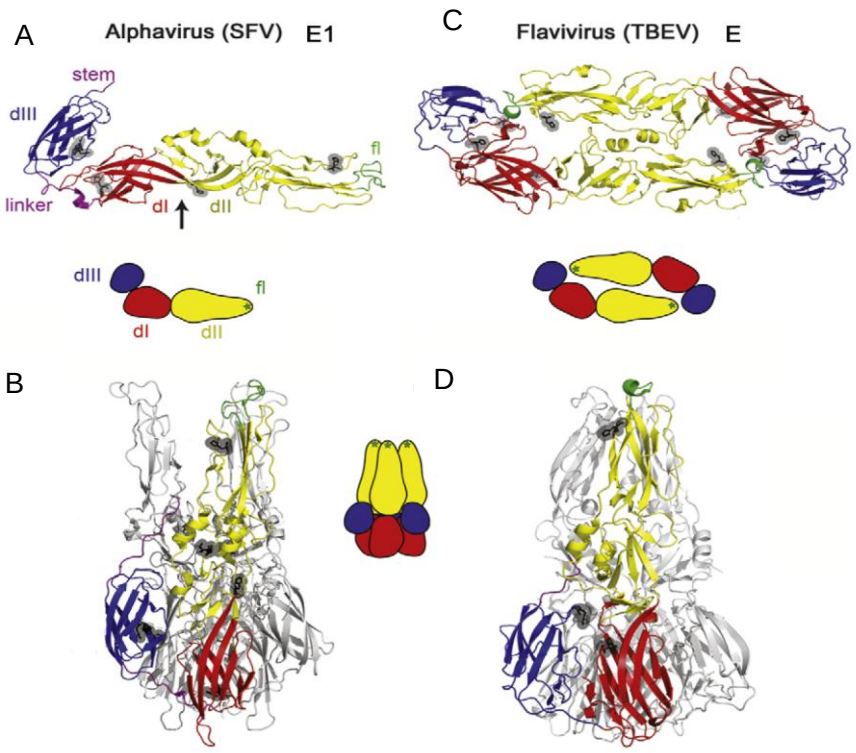

Figure 13 Ribbon diagrams and schematic representations of flavivirus (TBEV) and alphavirus (SFV) fusion proteins. Pre-fusion conformation (A, C) and postfusion conformation (B, D) of the E1 (SFV) and the E (TBEV) ectodomain. Color code: DI in red, DII in yellow, DIII in blue, fusion peptide (fp) in green. (Figure adapted from (Sanchez-San Martin et al., 2009))

2.4 Expression of Recombinant Flavivirus Proteins

Various methods for the expression of recombinant proteins of flaviviruses have been described (Allison et al., 1995b; Altmann et al., 1999; Bressanelli et al., 2004; Demain and Vaishnav, 2009; Hacker et al., 2009; Heinz et al., 1995; Jaiswal et al., 2004; Lieberman et al., 2007; Liu et al., 2010; Maroni et al., 1986; Modis et al., 2003; Modis et al., 2004; Modis et al., 2005; Sugrue et al., 1997a; Sugrue et al., 1997b; Tripathi et al., 2008; Volk et al., 2007; Volk et al., 2009; Zhang et al., 2004).

The choice of the appropriate expression system depends on the yield and on the particular requirements of the protein to obtain it in its native structure. Specific characteristics such as posttranslational modifications (disulphide bridges and glycosylation) determine the proper folding of a protein and are crucial for its function. For glycosylation eukaryotic cells are obligate. Naturally, flaviviruses replicate in mammalian and insect cells. Therefore these cell lines are suitable for the correct expression of recombinant proteins.

2.4.1 Expression of recombinant proteins in bacterial expression systems

For the production of recombinant proteins, the most commonly used bacterium is *Escherichia coli* (*E. coli*) (Demain and Vaishnav, 2009). *E. coli* is an inexpensive system and its genetics are well understood. Its genome can be easily and precisely modified. Rapid expression and high yields of the desired protein are additional advantages (Demain and Vaishnav, 2009). Drawbacks are the possible expression of proteins in inclusion bodies and the missing posttranslational modifications. The bacterial expression system is therefore mainly used for bacterial proteins. However, for some mammalian proteins the posttranslational modification can be neglected like γ-interferon (Demain and Vaishnav, 2009). Bacterial expression of DIII in its native fold was shown for WNV (Volk et al., 2004; Zlatkovic et al., 2011) YFV (Volk et al., 2009), DENV (Jaiswal et al., 2004; Tripathi et al., 2008; Volk et al., 2007; Volk et al., 2009) and Omsk hemorrhagic fever virus (Volk et al., 2006).

2.4.2 Expression of recombinant proteins in yeast expression systems

Yeast is a eukaryotic fungal organism that is often used for protein expression due to costefficient high production of recombinant proteins. A further advantage is the secretion of expressed proteins. *Saccharomyces cervisiae* and *Pichia pastoris* are the most commonly used strains and are genetically well characterized. Protein processing and posttranslational modifications are similar to mammalian cells. Yeast strains can assist protein folding and handle disulphide bridge rich proteins. In contrast to mammalian cells, yeast produces o-linked oligosaccharides containing only mannose and not sialylated o-linked chains (Demain and Vaishnav, 2009). The production of recombinant DENV E protein in *Pichia pastoris* was not successful due to proteolytic degradation (Sugrue et al., 1997a), but immunogenic DENV 1 virus-like particles (VLPs) could be produced, although *Pichia pastoris* was unable to modify one of the two available glycosylation sites (Sugrue et al., 1997b).The production of VLPs was also successful for DENV 2 (Liu et al., 2010)

2.4.3 Expression of recombinant proteins in insect expression systems

The moderate growth rate of insect cells is a shortcoming of the insect expression system. Still, it is a favourable expression system for the production of mammalian proteins due to high expression rates and fast and easy scale up. Posttranslational modifications are similar to mammalian cells (Demain and Vaishnav, 2009), although insect cells differ particularly in N-glycosylation from mammalian cells (Altmann et al., 1999; Hacker et al., 2009; Kim et al., 2005). Two systems were used for flavivirus protein production: the baculovirus expression system and the *Drosophila* expression system (DES). In the baculovirus expression system, *Spodoptera frugiperda* cells are used (Demain and Vaishnav, 2009). In DES, an inducible expression of stable cell lines is possible, for the use of a metallothionein promotor and heavy metals for induction (Maroni et al., 1986).

The insect expression system is therefore well suited for the production of flavivirus proteins. Several proteins have been successfully produced, among them the WNV sE with a baculovirus shuttle vector in Hi-5 insect cells (Nybakken et al., 2006), sE of WNV (Lieberman et al., 2007; Zlatkovic et al., 2011), sE of TBEV

(Zlatkovic et al., 2011) and sE of DENV 2 and DENV 3 (Modis et al., 2003; Modis et al., 2004; Modis et al., 2005) in the DES system.

2.4.4 Expression of recombinant proteins in mammalian expression systems

Expression in mammalian expression systems guarantees proper folding, addition of fatty acid chains, production of complex glycans and phosphorylations (Demain and Vaishnav, 2009; Hacker et al., 2009) that insect expression cells cannot accomplish.

Poor secretion, long incubation periods and high costs are the downside.

The expression of flaviviral proteins is well established in various mammalian cell lines. Recombinant subviral particles (RSPs) of JEV& DENV 1-4 (Konishi et al., 1992; Mason et al., 1991; Wang et al., 2009) have been produced in HeLa cells with a recombinant vaccinia virus encoding prM and E genes. Furthermore, VLPs of WNV have been generated in CHO cells (Ohtaki et al., 2010) and DENV VLPs were expressed in COS-1 (Crill et al., 2009).The expression of TBEV E protein, sE protein and RSPs has been established in COS-1 cells (Allison et al., 1995b; Heinz et al., 1995; Schalich et al., 1996) and VLPs of JEV in RK13 cells (Kojima et al., 2003).

3 Objectives

The final postfusion structure of a soluble fragment of the fusion protein E (sE) is known, but important elements (including the two helices of the stem region and the transmembrane anchor) have not been resolved. According to the fusion model, the “zippering” of the stem along DII during the conformational changes of E might be important for the formation of a hemifusion intermediate and the stable hairpin-like postfusion trimer. Modeling studies allowed the positioning of the first helix (H1) into the truncated postfusion structure of sE, but it was not possible to place the second helix (H2), indicating that – in the presence of the stem – the postfusion structure could be different. It was therefore the aim of this thesis to generate and characterize different recombinant postfusion sE trimers of tick borne encephalitis virus: 1) sE with the first helix (sEH1) 2) sE with helix1 and a truncated stem helix 2 (lacking the last four carboxy-terminal residues of helix 2; sEH1H2 $_{444}$) and 3) sE with both stem helices (sEH1H2 $_{448}$). Using the *Drosophila* expression system (DES), Schneider S2 cell lines that stably express TBE virus sEH1, sEH1H2 $_{444}$ and sEH1H2 $_{448}$ fused to a cleavable protein tag will be established. Purification and conversion into the trimeric postfusion forms will be carried out as described previously. The obtained postfusion trimers will be characterized and - after large scale expression and purification – can be further used for the determination of their X-ray crystal structures. This should lead to new insights into the role of the stem region during the membrane fusion process, thus contributing to the understanding of the flavivirus fusion mechanism.

4 Material and Methods

4.1 Manipulation of nucleic acids

4.1.1 Plasmids

For the production of recombinant TBEV sE proteins in the *Drosophila* Expression System (DES), the expression plasmid pT389-sEH1H2 $_{448\ dstrep}$ was used (Geller, 2009). This expression plasmid pT389-sEH1H2 $_{448\ dstrep}$ consists of the pT389 vector with an expression cassette, containing the sequence encoding the prM and the E protein (amino acids 1-448) of TBEV strain Neudoerfl (Mandl et al., 1988). The pT389 vector (provided by the Institut Pasteur, France) contains the Drosophila signal sequence Bip that is important for secretion of the target proteins, a pUC origin for replication in bacterial cells, a metallothionin (MT) promoter for inducible expression of target genes (Invitrogen TM, Life Technologies) (Bunch et al., 1988; Maroni et al., 1986), an ampicillin resistance for selection in bacterial cells, an enterokinase cleavage site and two strep tags for purification of the target protein.

4.1.2 DNA digestion and restriction enzymes

For digestion of vector pT389-sEH1H2 $_{448\ dstrep}$ and the synthesized plasmid, sEH1H2_del, 2µg DNA were incubated with the enzymes *Apa*I and *Pas*I (Fermentas) according to manufacturer's protocols. The restriction was controlled by agarose gel electrophoresis (4.1.3).

4.1.3 Agarose gel electrophoresis

DNA fragments were separated on a 1% (w/v) agarose gel containing 2.5µg/ml ethidium bromide. *Lambda phage* digested with *Hind*III (fragment sizes in bp: 23130, 9416, 6557, 4361, 2322, 2027, 564 and 125) was used as a size marker. DNA fragments were separated for 30-50 minutes at 120V and visualized, using a trans-illuminator at a wavelength of 320nm.

4.1.4 Preparative agarose gel and DNA extraction

For purification of DNA fragments after digestion, an agarose gel electrophoresis was performed as described in 4.1.3, using the whole digestion mix. The desired bands were excised from the gel under UV light and DNA was extracted with Wizard® SV Gel and PCR Clean-Up System purchased from Promega.

4.1.5 Ligation

Ligation of DNA fragments was performed with T4 DNA Ligase (Fermentas) at a ratio of 5:1 of insert and vector. The reaction mix was incubated at room temperature for ten minutes and directly used for the transformation of chemically competent *Escherichia coli* cells (4.1.7).

4.1.6 Site Directed Mutagenesis

In order to generate sEH1H2 constructs without a strep tag (sEH1H2) or with a single strep tag (sEH1H2 $_{strep}$), site directed mutagenesis (GeneTailor™ Site-Directed Mutagenesis System from Invitrogen™) was performed according to the manufacturer's protocol. The sequences of the primers (VBC Biotech Services GmbH) used for the mutagenesis PCR and the PCR conditions are listed in table 1 and 2. All expression plasmids were amplified in *Escherichia* coli strain DH5α-T1^{R} (4.1.7-4.1.8) and the sequences were controlled (4.1.10) before expression in *Drosophila* Schneider 2 cells (4.2).

Table 1 Conditions for PCR reaction

sEH1H2 $_{STOP}$				sEH1H2 $_{STREP}$			
Initial denaturation	98 °C	2’		**Initial denaturation**	98 °C	2’	
Denaturation	98 °C	30’’	**20x**	**Denaturation**	98 °C	30’’	20x
Annealing	65 °C	30’’		**Annealing**	68 °C	30’’	
Extension	68 °C	6’		**Extension**	72 °C	6’	
Final Extension	68 °C	10’		**Final Extension**	72 °C	10’	
End	4 °C	∞		**End**	4 °C	∞	

Table 2 Primers used for site directed mutagenesis PCR

	Forward Primer 5’ →3’	Reverse Primer 5’ →3’
sEH1H2 $_{444\ STOP}$	CCTTGGTGGCGCTTAAGGGCCCTTC	AGCGCCACCAAGGACCGTATGTAC
sEH1H2 $_{448\ STOP}$	GCTTTCAACAGCATCTAAGGGCCCTTC	GATGCTGTTGAAAGCGCCACCAAGG
sEH1H2 $_{444\ SSTREP}$	TCCACAATTCGAGAAGTGAGTTTGAGGCGGCGG	TTCTCGAATTGTGGATGACTCCAACCGGCC
sEH1H2 $_{448\ SSTREP}$	TCCACAATTCGAGAAGTGAGTTTGAGGCGGCGG	TTCTCGAATTGTGGATGACTCCAACCGGCC

4.1.7 Transformation of chemically competent bacteria

50µl of DH5α-T1^{R} competent *E. coli* (Invitrogen) were transformed with 5µl DNA according to the manufacturer´s protocol. Transformed bacteria cells were plated on LB plates, containing ampicillin (LB $^{+amp}$) to select bacteria carrying the ampicillin resistance gene in the vector. Plates were incubated overnight (16 h) at 37°C to allow bacterial growth.

LB medium	10g Bacto tryptone
	5g Yeast extract
	10g NaCl
	ddH_2O to a final volume of 1 liter
	adjusted to pH 7.0 with NaOH

LB $^{+amp}$ medium	LB medium, containing 100µg/ml ampicillin
LB agar medium	LB medium, containing 20g/l difco agar

4.1.8 Plasmid preparation

Single E.coli colonies grown on LB $^{+amp}$ plates were picked to inoculate liquid LB^{+amp} medium. These cultures were harvested after 16 h at 37°C under shaking conditions. DNA was purified in small scale either with the PureYield™ Plasmid Miniprep System (Promega) or the PureYield™ Plasmid Midiprep System (Promega) according to the manufacturer´s protocol. If ethanol was retained in the sample after purification, ethanol was precipitated as explained in 4.1.9.

The concentration of DNA was determined with the Nano Drop 1000 (Peqlab).

4.1.9 Ethanol precipitation of DNA

DNA samples were mixed with 1/10 volume sodium acetate (pH=5.2) and three volumes of 96% ethanol. The mixture was incubated for 15 minutes at -20°C. DNA was pelleted by centrifugation at 14,000 rpm (Eppendorf, 5417R) for 20 minutes at 4°C. Afterwards the DNA pellet was washed with cooled 70% ethanol and dried for several minutes prior to resuspension in nuclease free ddH_2O.

4.1.10 DNA sequencing

Sequence analysis was carried out using the ABI Prism Big Dye Terminator Cycle Sequencing Kit according to the manual. 300-500ng DNA and 6pmol primer were added to 4µl Big Dye Ready Mix and filled up with nuclease free ddH_2O to a volume of 20µl. The reaction for DNA sequencing was performed with the settings shown in table 3.

Table 3 Settings for the reaction of DNA sequencing

Reaction Settings			
Initial denaturation	96 °C	20''	
Denaturation	96 °C	30''	35x
Annealing	50 °C	15''	
Extension	60 °C	4'	
End	4 °C	∞	

The amplified, labeled DNA products were purified by centrifugation through swelled Sephadex plates and were analyzed by an automatic capillary sequencer (Applied Biosystems, GA 3100). The results were evaluated with the software Geneious Pro™ 5.3 (Drummond AJ, 2011).

4.2 Cell culture

4.2.1 Drosophila melanogaster Expression System (DES)

The DES was developed by the SmithKline Beecham Corporation and is proprietary to this company. The DES is licensed to Invitrogen Corporation. Materials of the kit are the subject of U.S. Patents No. 5,5500,043, 5,681,713 and 5,705,359.

The *Drosophila melanogaster* Schneider 2 cell line (S2 cell line) from Invitrogen was maintained in Schneider's complete *Drosophila* medium (Fisher Scientific) with 10% fetal calf serum (FCS) and 1% antibiotic antimycotic solution (penicillin, streptomycin and amphotericin B) purchased from Gibco. Selection medium included 25*µ*g/ml Blasticidin (Fisher Scientific). For protein expression, serum-free medium (Lonza) with 1% antibiotic antimycotic solution (penicillin, streptomycin and amphotericin B) and 10*µ*g/ml Blasticidin (Fisher Scientific) was used.

4.2.2 Stable transfection of S2 cells

In order to stably transfect S2 cells, cultures were grown in 6-well plates to a density of 2-4x10^6 cells/ml. A reaction mix of 36µl 2M $CaCl_2$, 1µg selection vector pCoBlast and 19µg recombinant DNA in a volume of 300µl was dropwise added to 300µl 2xHBS and incubated at room temperature for 40 minutes. The mix was added to the S2 cells and cells were incubated at 28°C for 24 h. Subsequently, cells were washed twice with Schneider's complete *Drosophila* medium. Cells were washed by centrifugation at 100g for 10 minutes and resuspended in fresh medium. After 48h at 28°C cells were selected by changing medium to selection medium containing Blasticidin. Every two days, medium was exchanged and the cell density was measured until resistant cells started growing. After approximately three weeks of selection, stably transfected cell lines were obtained.

4.2.3 Subculturing of S2 cells

S2 cells were grown in complete selection medium at 28°C and split at a cell density of $1x10^7$ cells/ml. To adapt cells to serum free medium, S2 cells were consecutively split into medium with 50%, 75% and finally 100% serum free medium and grown in shaking suspension cultures at 28°C.

Cells were counted with Nexelcom Bioscience Cellometer Auto T4.

4.2.4 Protein expression and purification

4.2.4.1 Optimization of induction of protein expression

To optimize protein expression transfected cells were grown to a density of $2x10^6$ cells/ml and expression was induced with 0mM, 0.75mM, 1.0mM or 1.25mM $CuSO_4$. Samples were taken at different time points after induction until the cell density reached $1\text{-}2x10^7$ cells/ml, typically after seven to nine days. Protein expression was measured by a quantitative four-layer ELISA, described in 4.3.2.1.

4.2.4.2 Expression of protein

Stably transfected cells were adapted to serum free medium (4.2.3) and seeded at a density of $2\ x10^6$cells/ml. Protein expression was induced with 1.0mM $CuSO_4$. 500ml of cell suspension were incubated seven to nine days under shaking conditions until the cell density reached about $1x10^7$cells/ml. Afterwards the cell culture supernatant (in the presence or absence of detergent) was cleared by centrifugation at 4,000g for 30 minutes at room temperature and filtration through a 0.22µM filter (Steritop,VWR). The cleared supernatant was concentrated to 1/5 of the original volume using Vivaflow 200 system (Sartorius) according to the manufacturer's protocol.

4.2.4.3 Purification

4.2.4.3.1 Cation ion exchange chromatography (IEX)

Concentrated cell culture supernatant containing tag-less recombinant sE was subjected to cation ion exchange chromatography using HITRAP SP FF columns (GE Healthcare) and the ÄKTA fast protein liquid chromatography (FPLC) system from GE Healthcare. The medium was exchanged to 20mM MES, pH=6.1, 0.5% DDM (Sigma Aldrich ®) with PD-10 (GE Healthcare) desalting columns prior to purification. Then, the protein was applied to the column and washed with 20mM MES pH=6.1, 1M NaCl to remove unspecifically bound protein. The protein was eluted with a linear NaCl gradient (0- 2M NaCl in a buffer of 10mM MES pH=6.1; 0.5% DDM) and collected in 1 ml fractions.

4.2.4.3.2 Small scale purification by affinity chromatography with streptactin

Concentrated cell culture supernatant (pH=7.5) (4.2.4.2) was mixed with avidin to a final concentration of 15µg/ml and subjected to an equilibrated streptactin spin column (Biotag). The recombinant protein bound to the column matrix via its strep tag. The column was washed with 400µl buffer W pH=8.0 (100mM Tris/HCl; 150mM NaCl; 1mM EDTA) and recombinant protein was eluted with buffer W pH=8.0, containing 2mM D-Biotin. All steps were carried out according to the manufacturer's protocol.

4.3 Biochemical characterization

4.3.1 Coflotation assay

4.3.1.1 Liposome Production and Extrusion

Phosphatidylcholine (PC), phosphatidylethanolamine (PE) (Avanti Polar Lipids) and cholesterol (Sigma) were mixed in a ratio of 1:1:2 from stock solutions in chloroform. The mixture was dried to a thin film using a rotary evaporator and then dried further in high vacuum for at least 1.5h. The lipid film was hydrated in 10mM

triethanolamine (pH=8.0), 140mM NaCl and subjected to five cycles of freeze-thawing, followed by 21 cycles of extrusion through two polycarbonate membranes with a pore size of 200nm using a Lipofast syringe-type extruder (Avestin, Ottawa, Canada).

4.3.1.2 Enterokinase (EK) cleavage

Cleavage was carried out for 30 minutes at 4°C at a ratio of protein to enzyme of 1µg sE to 0.05 units EK.

4.3.1.3 Coflotation

Purified sEH1 was acidified with MES to a pH of 5.4 in the presence of liposomes (at a ratio of 1µg sE to 15nMol Lipid). The mixture was incubated for 30 minutes at 37°C, adjusted to 20% sucrose and loaded on a 50% sucrose cushion. It was overlaid with 15% and 5% sucrose. All sucrose solutions were prepared in TAN buffer pH=8.0. After 1.5h centrifugation at 4°C and 50,000 rpm (SW 55 Beckman Coulter rotor), the top fraction was harvested and the amount of protein was determined by a quantitative four-layer ELISA (described in 4.3.2.1).

4.3.2 ELISA

4.3.2.1 Quantitative four-layer ELISA

96 well microtiter plates (Nunc Maxisorp Microtiter plates) were coated with polyclonal guinea pig anti-flavivirus IgG (2,5µg/ml in carbonat coating buffer pH 9.6) for 2-4 days at 4°C in a humid chamber. Purified TBEV (strain Neudoerfl) or sE protein were used as internal standards. Samples and standard were denatured with 0.4% sodium dodecyl sulfate (SDS) at 65°C and then diluted in ELISA buffer. Aliquots of 50µl of sample were applied to the microtiter plates and incubated for 1.5h at 37°C in a humid chamber. After washing the plates four times with washing buffer,

rabbit anti-TBEV serum was added, incubated for 1h at 37°C and then washed again. A donkey anti-rabbit IgG, peroxidase-linked antibody and O-phenyldiamine as substrate were used for detection as described previously (Heinz et al., 1994). The reaction was stopped with 2N H_2SO_4. Absorbance was measured at 490/630nm in a multichannel photometer and concentrations were determined with the KCjunior software (BioTek). Used antibodies are listed in table 4.

Table 4 Antibodies used in Quantitative four-layer ELISA

Antibody	Type of Ab	Company	Concentration
Guinea pig anti-flavivirus IgG	polyclonal		2.5 µg/ml
Rabbit anti-TBEV serum	polyclonal		Lot-dependent
Donkey anti-rabbit IgG, peroxidase-linked species-specific whole antibody	polyclonal	GE Healthcare	Lot-dependent

4.3.2.2 Conformational analysis by ELISA

The conformation of different trimers was investigated with monoclonal antibodies (mabs). 96 well microtiter plates (Nunc Maxisorp Microtiter plates) were coated with 1µg/ml protein specific mabs (4G2 or B2) in carbonate coating buffer pH 9.6 for two days at 4°C in a humid chamber. Trimer preparations were serially diluted in ELISA buffer from 1 to 0.000333µg/ml, applied to the plates and incubated for 1.5h at 37°C in a humid chamber. Further procedures as described in 4.3.2.1. Used antibodies are listed in table 5.

Table 5 Antibodies used in Conformational analysis by ELISA

Antibody	Type of Ab	Company	Concentration
4G2	monoclonal		1 µg/ml
B2	monoclonal		1 µg/ml
Rabbit anti-TBEV serum	polyclonal		Lot- dependent
Donkey anti-rabbit IgG, peroxidase-linked species-specific whole antibody	polyclonal	GE Healthcare	Lot dependent

4.3.2.3 ELISA buffers

0,05M Carbonate buffer pH=9,6	1.59g Na_2CO_3 2.93g $NaHCO_3$ H_2O_{dd} to a final volume of 1l
PBS pH=7.4	137mM NaCl 1.76mM KH_2PO_4 10mM Na_2HPO_4*12 H_2O 2.7mM KCl
ELISA buffer	PBS pH=7.4 2% Tween-20 2% Lamb serum
Washing buffer	PBS pH=7.4 0.05% Tween-20
Peroxidase Substrat Phosphat-Citrat buffer pH=5.0	1mg/ml o-Phenylendiamin (OPD) in 90% 0.11M Na_2HPO_4*2 H_2O 10% 0.5M $C_6H_8O_7$* H_2O 0.3% H_2O_2

4.3.3 Sedimentation analysis

The oligomeric state of sE proteins was measured by sedimentation analysis as described previously (Allison et al., 1995a). As controls, solubilized low-pH-pretreated (E trimer control) and untreated (dimer control) virus preparations were included (Allison et al., 1995a). 3µg sE, solubilized virus-derived E trimers and E dimers in TAN buffer pH 8.0 containing detergent (e.g. 0.5-1% Triton X-100) were applied to 7 to 20% continuous sucrose gradients containing 0.1% Triton X-100. Samples were centrifuged for 20h in an SW 40 rotor (Beckman) at 38,000rpm and 15°C. Fractions were collected by upward displacement (Biocomp Piston Fractionator), and E protein was determined by a quantitative four-layer ELISA after denaturation with 0.4% SDS (4.3.2.1).

4.3.4 Chemical cross-linking with DMS

E protein-containing fractions from sedimentation analyses were subjected to cross-linking with 10mM dimethylsuberimidate (DMS) for 30 minutes at room

temperature as described previously (Allison et al., 1995a). The reaction was stopped by the addition of ethanolamine to a final concentration of 10mM. The cross-linked samples were precipitated as described (4.3.5) and separated by electrophoresis on 5% SDS polyacrylamide gels using a phosphate-buffered system (4.3.7), blotted onto polyvinylidene difluoride membranes (Bio-Rad) using a Bio-Rad Trans-Blot semidry transfer cell, and detected and visualized immunoenzymatically (4.3.8)

4.3.5 Protein precipitation with deoxycholic acid (DOC) and tricholoracetic acid (TCA)

Protein solutions (with or without prior cross-linking) were incubated with 0.0015% DOC for 30 minutes at room temperature and then precipitated with 8% TCA overnight on ice, followed by centrifugation for 10 minutes at 14,000g and 4°C. The pellet was washed three times with ice cold acetone (14,000g, 10 minutes, 4°C) and dissolved in 20µl of the respective sample buffer

4.3.6 SDS-Polyacrylamide gel electrophoresis (SDS-PAGE) according to Laemmli

The electrophoresis was performed at 20 mA/gel using 0.75 mm thick gels with a 3% stacking gel and a 12% or 15% separation gel. A pre-stained rainbow molecular weight marker (high range RN756E – 225; 76; 52; 38; 31; 24; 17; 12 kDa) from GE Healthcare was used.

For staining, the gels were shaken for 30 minutes in the fixation solution and then for 30 minutes in the Coomassie solution. After destaining, the gel was dried using a gel dryer (Model 543, BioRad) according to the manufacturer's instruction.

3% stacking gel	385µl 40% Acrylamide
	625µl 1M Tris (pH=6.8)
	3.92ml ddH_2O
	50µl 10% SDS
	25µl Ammonium persulfate (APS)
	5µl N,N,N´,N´-tetramethyl-ethylendiamine (TEMED)

15% separation gel	1.88ml 40% Acrylamide
	1.25ml 1,5M Tris (pH=8.8)
	1.8ml ddH_2O
	50µl 10% SDS
	25µl APS
	5µl TEMED
Laemmli sample buffer	0.125M Tris (pH=6.8)
	2% SDS
	10% Glycine
	0.0025% Bromphenol blue
	5% ß-Mercaptoethanol
5x Running buffer	60g Tris
	288g Glycine
	ddH_2O to a final volume of 2000 ml
	0,1% SDS prior to use
Fixation solution	50% (v/v) Ethanol
	10% (v/v) Acetic acid
Coomassie solution	0.1% (w/v) Coomassie blue R350
	20% (v/v) Methanol
	10% (v/v) Acetic acid
Destaining solution	50% Methanol
	10% Acetic acid

4.3.7 SDS-PAGE according to Maizel

The electrophoresis was performed at 20 mA/gel using 0.75 mm thick 5% gels. A pre-stained rainbow molecular weight marker (complete range RNP800E – 225; 150; 102; 76; 52; 38; 31; 24; 17; 12 kDa) from GE Healthcare was used.

Gels were used for semidry western blotting as described in 4.3.8

5% gel (5ml)	625µl 40% Acrylamide
	500µl 1M Sodium-Phosphate
	3.795ml ddH_2O
	50µl 10% SDS
	25µl APS
	5µl TEMED
Sample buffer (10ml)	2ml 10%SDS
	1.15ml Glycerine
	250µl Bromphenolblue (1%)
	100µl 1M Sodium-Phosphate
	6.5ml ddH_2O
Running buffer	0.1M Sodium-Phosphate
	0.1% SDS

4.3.8 Semidry Western blotting

0,3µg-1µg purified protein or virus were subjected to SDS-PAGE as described above. A polyvinyldifluoride (PVDF, BioRad) membrane was soaked in methanol (Merck) for 5 minutes and then- together with the gel- equilibrated in blotting buffer. The proteins were transferred for 1.5h at 18V onto the PVDF membrane with a Semidry Transfer Cell from BioRad. The membrane was blocked overnight at 4°C with 1% bovine serum albumin in PBS pH= 7.4 containing 0.1% Tween-20. The respective primary antibody (Table 6), diluted in blocking buffer, was added for 2h at room temperature. The membrane was washed and incubated with the peroxidase-labeled IgG-specific secondary antibody for 1.5h at room temperature. The substrate reaction was carried out with the SIGMAFAST^{TM} DAB tablets. Used antibodies are listed in table 6.

Table 6 Antibodies used in Semidry Western blotting

	Primary antibody
Anti Strep Tag Western blot	Monoclonal anti-strep tagII
Western blot to visualize Crosslinking assay	Polyclonal rabbit anti-TBEV serum KP-M2

Blotting buffer	5.82g Tris
	2.93g glycine
	3.75ml 10% SDS
	200ml Methanol
	ddH_2O to a final volume of 1l
Blocking buffer	1% BSA
	0.2% Tween-20
	in PBS pH=7.4

5 Results

5.1 Generation of sE trimers containing helix 1 of the stem region (sEH1)

Purified sEH1 dimers containing double strep tag (sEH1 $_{dstrep}$), produced in stably transfected *Drosophila* S2 cells, were previously used for trimer productions (Geller, 2009) (unpublished data). Unfortunately, the sE trimers did not crystallize (unpublished data). Therefore, tag-less sEH1 trimers were generated in this diploma thesis. For this purpose, purified sEH1 dimers were cleaved with enterokinase to remove the strep tag and acidified in the presence of liposomes to induce trimerization (Material and Methods). Subsequently, liposome-associated trimers were separated from unbound material by centrifugation in sucrose step gradients (Material and Methods). The top fraction, containing the liposome bound trimers, was solubilized with detergent and lipids were removed by ultrafiltration (Material and Methods). To exclude tag-containing trimers that might still be present in the preparations, the trimers were subjected to a small-scale streptactin affinity chromatography, using spin columns (Material and Methods). Typically, the recovery of tag-less sEH1 trimers was about 40-50% of the input material. A representative example of the procedure is shown in figure 13.

To confirm the trimeric state of the final product, a sedimentation analysis in the presence of detergent was carried out. As shown in figure 14, the protein was exclusively found in the fractions corresponding to a trimer.

To determine the homogeneity and the removal of the tag of the sEH1 trimer, an SDS-PAGE and a Western blot using a strep tag-specific monoclonal antibody were carried out. As controls, sEH1 dimers (before and after partial enterokinase cleavage of the strep tag), and TBEV were included. In the case of the sEH1 trimer, most of the protein migrated as a single band at the expected size (Figure 15 A) and did not react with the monoclonal antibody (Figure 15 B) indicating that the tag-removal was successful.

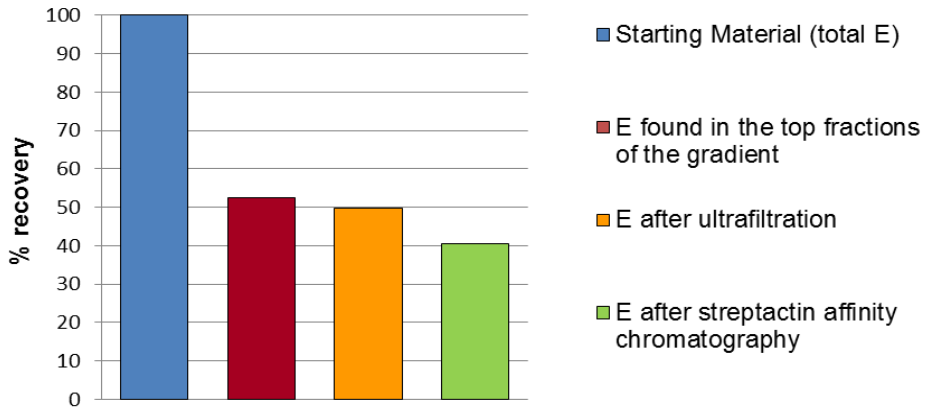

Figure 13 Recovery diagram of sEH1 trimer conversion. Samples were quantified by a four-layer ELISA.

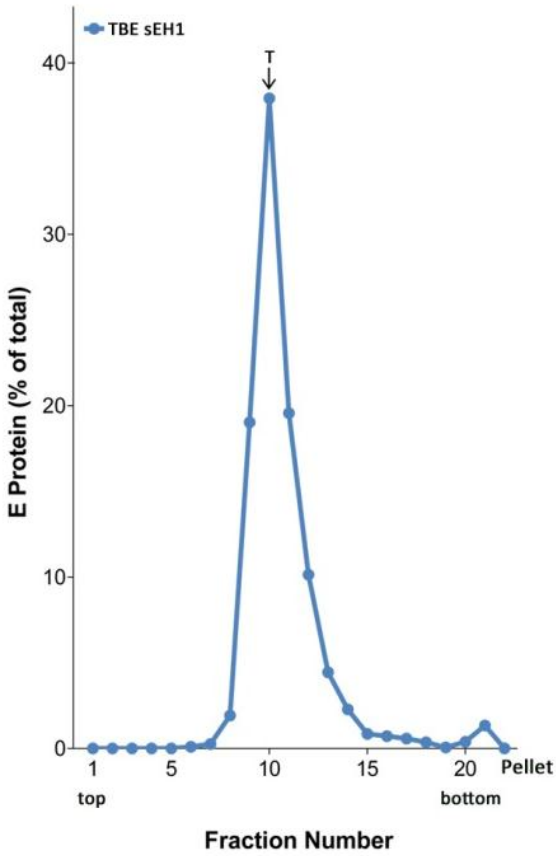

Figure 14 Sedimentation analysis of sEH1 trimers in the presence of detergent. The sedimentation direction is indicated from left to right. The position of the trimer (T) is highlighted.

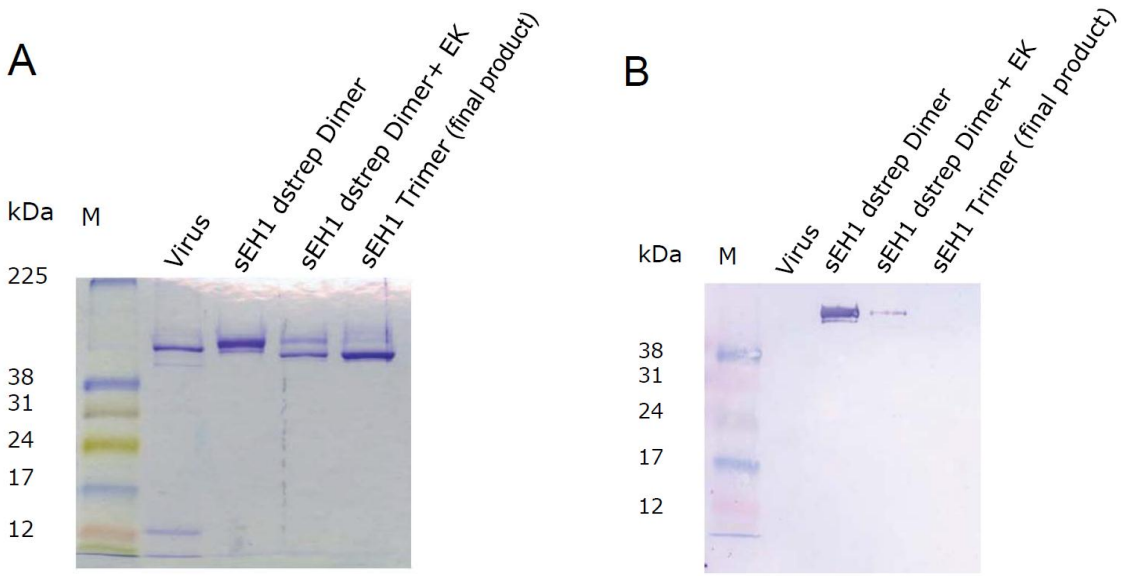

Figure 15 (A) Coomassie-stained 12% SDS-PAGE and **(B)** Western blot using an anti-strep-tag mab. TBEV and TBE sEH1 $_{dstrep}$ dimer were used as controls.

EK: Enterokinase

TBE sEH1Trimer: Final trimer preparation

M: Marker

5.2 Generation of sE trimers containing the stem region (sEH1H2)

The first attempts to purify recombinant sEH1H2 proteins containing the whole stem region and a double strep tag from stably transfected *Drosophila* S2 cells was unsuccessful (unpublished data). The recovery of the protein after purification using streptactin affinity chromatography was below 10% (unpublished data). The experiments indicated that the increase in hydrophobicity of sEH1H2 compared to sEH1 led to aggregation of the proteins in the cell culture supernatant and impaired their binding to streptactin. Furthermore, the elution of the (probably aggregated) and via the strep-tag bound sEH1H2 proteins was very inefficient (unpublished results). Therefore, new constructs were designed for the production of sEH1H2 proteins using the *Drosophila* expression system (Figure 16). 1) The last 4 amino acids of helix 2 were deleted to decrease the hydrophobicity of the protein (sEH1H2 $_{444\ dstrep}$), 2) the second strep tag was deleted to facilitate elution from the streptactin columns (sEH1H2 $_{448\ strep}$ and sEH1H2 $_{444\ strep}$), and 3) the strep tag was deleted completely

(sEH1H2 $_{448}$ and sEH1H2 $_{444}$). For the sEH1H2 proteins without tag other purification strategies such as ion-exchange chromatography had to be established.

All new expression plasmids were based on the already existing sEH1H2 $_{448\ dstrep}$ construct (Geller, 2009) (Figure 16) (Material and Methods).

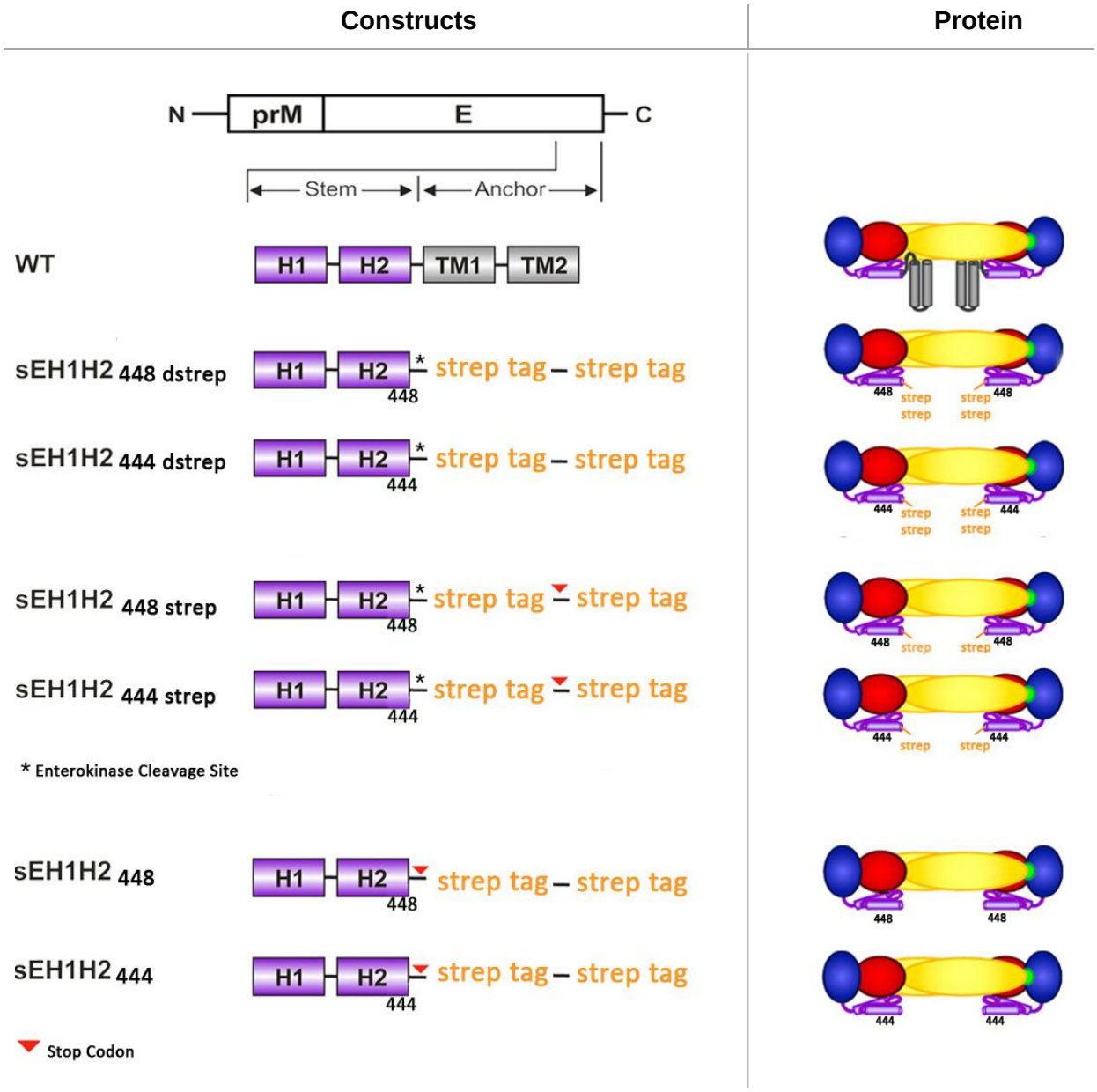

Figure 16 Schematic representations of the C-terminal truncation and modification of recombinant E proteins. The schematic shows details of the flavivirus genome organization in the corresponding constructs (left panel) and the resulting E proteins (right panel)
WT: wildtype E protein with the stem–anchor region (496 amino acids)
sEH1H2 $_{448}$: contains the whole stem region (448 amino acids)
sEH1H2 $_{444}$: *sEH1H2* $_{448}$ without the last four amino acids (444 amino acids)
Color code: DI red, DII yellow with the fusion peptide in green, DIII blue, stem region purple, transmembrane anchor grey, red triangle symbolizes ATG stop codon, black asterisk enterokinase cleavage site.

5.2.1 Production of expression plasmids

5.2.1.1 Generation of the expression plasmid sEH1H2 $_{444}$ with a double strep tag (sEH1H2 $_{444\ dstrep}$)

To generate the plasmid encoding sEH1H2 $_{444}$ with a double strep tag (sEH1H2 $_{444\ dstrep}$), the 3'-terminal part of the gene coding for the E protein was synthesized (sEH1H2_del) (Figure 17). This region contains two unique restriction sites, PasI and ApaI. The expression vector sEH1H2 $_{448\ dstrep}$ and the synthesized vector were digested with the restriction enzymes ApaI and PasI (Figure 17) and the cleavage reactions were separated on an agarose gel (Figure 18). The appropriate gel fragments were isolated and ligated as described in Material and Methods. *E. coli DH5α* bacteria were transformed with the ligation product and selected on agarose plates containing ampicillin. Single colonies were picked and inoculated in medium for propagation. The DNA was isolated and the coding sequence was verified by sequencing (Material and Methods).

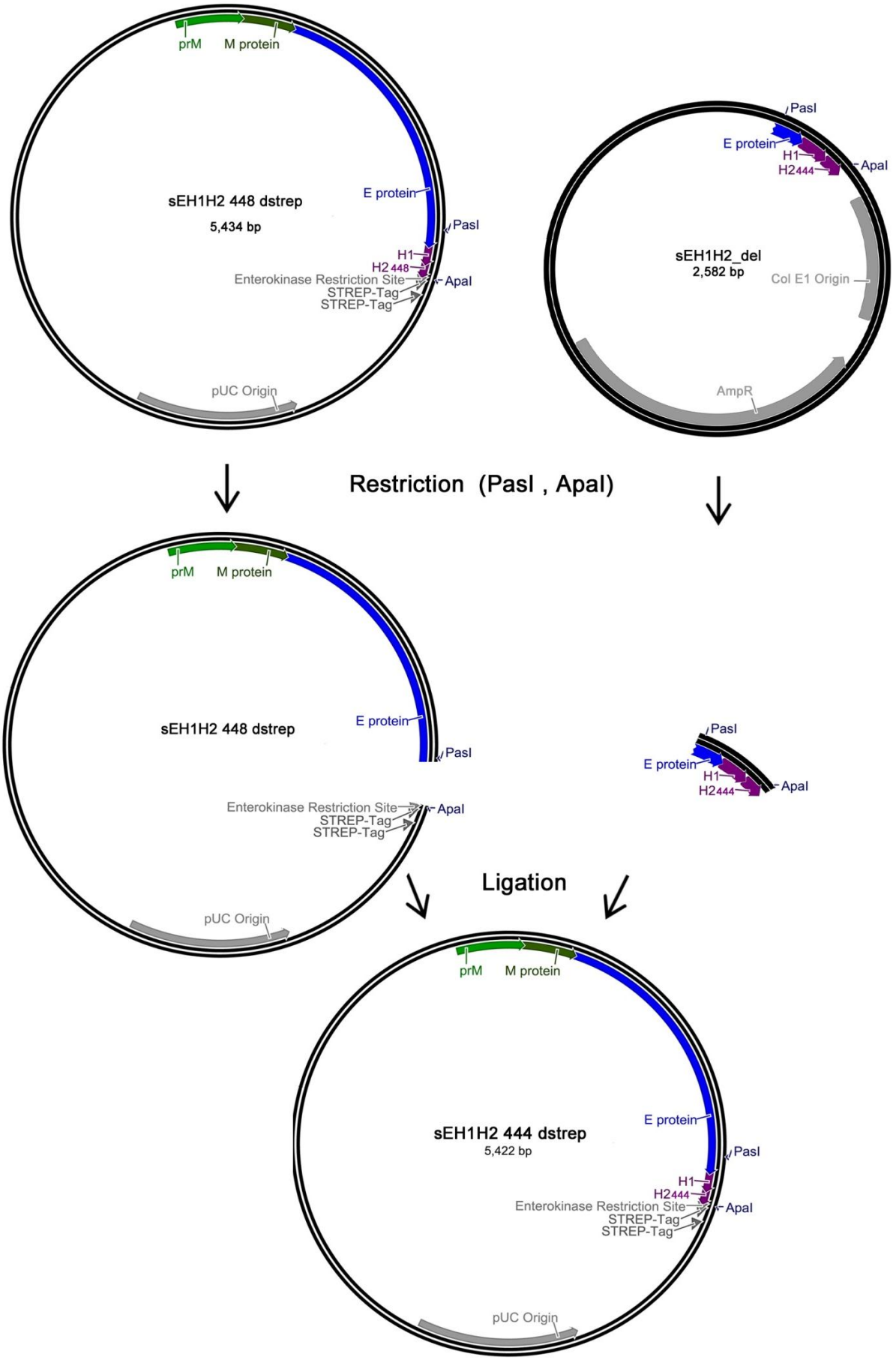
prM
M protein
sEH1H2 448 dstrep
5,434 bp
E protein
PasI
H1
H2 448
Enterokinase Restriction Site
ApaI
STREP-Tag
STREP-Tag
pUC Origin
PasI
E protein
H1
H2444
ApaI
sEH1H2_del
2,582 bp
Col E1 Origin
AmpR
Restriction (PasI , ApaI)
prM
M protein
sEH1H2 448 dstrep
E protein
PasI
Enterokinase Restriction Site
ApaI
STREP-Tag
STREP-Tag
pUC Origin
PasI
E protein
H1
H2444
ApaI
Ligation
prM
M protein
sEH1H2 444 dstrep
5,422 bp
E protein
PasI
H1
H2444
Enterokinase Restriction Site
ApaI
STREP-Tag
STREP-Tag
pUC Origin

Figure 17 Schematic representation of the cloning strategy of sEH1H2 $_{444\ dstrep}$. The expression vector sEH1H2 $_{448\ dstrep}$ and the synthesized plasmid sEH1H2_del, encoding for parts of the E protein and a shortened stem region (until amino acid 444), were cut with the restriction enzymes ApaI and PasI. The cut vector sEH1H2 $_{448\ dstrep}$ and the fragment sEH1H2_del were ligated. Color code: green the prM/M protein, blue the E protein, purple the stem region, grey restriction sites, the pUC origin and the double strep tag. Plasmids were drawn with Geneious v5.4 (Drummond AJ, 2011) and Photoshop.

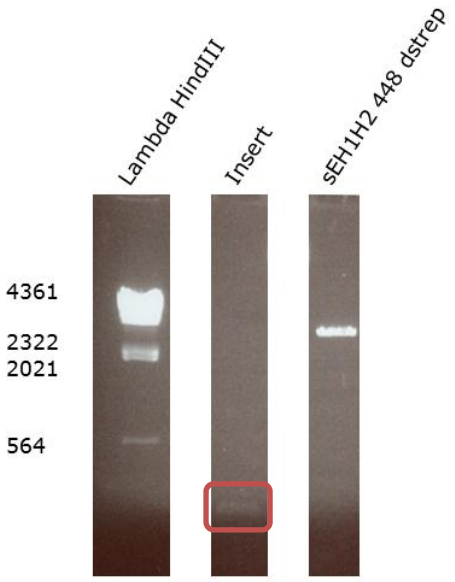

Figure 18 Analytical agarose gel electrophoresis of the cleaved insert of sEH1H2_del and the linearized expression vector sEH1H2 $_{448\ dstrep}$. The insert (205bp) and the vector (5217bp) were separated according to their molecular weight by a 1% agarose gel. The red rectangle highlights the insert at 205bp.

5.2.1.2 Generation of expression plasmids for sEH1H2 with single strep tag or without tag

To generate the expression vectors for sEH1H2 without tag (sEH1H2) or sEH1H2 with a single strep tag (sEH1H2 $_{sstrep}$), ATG stop codons were inserted at different positions of the expression plasmids by site directed mutagenesis PCR as described in Material and Methods. To obtain sEH1H2 without tag, an ATG stop codon was inserted after helix 2. To gain sEH1H2 with a single strep tag, an ATG

stop codon was inserted after the first strep tag. The PCR products were checked by sequencing (Material and Methods), which confirmed successful mutagenesis reactions.

5.2.2 Expression of recombinant sEH1H2 in *Drosophila melanogaster* S2 cells

5.2.2.1 Stable transfection of S2 cells and optimization of protein expression

For expression of the different recombinant proteins, *Drosophila melanogaster* Schneider S2 cells were cotransfected with the respective expression plasmid and the selection vector pCoBlast, with a Blasticidin resistance gene. Transfected cells were selected with medium (containing Blasticidin) for two weeks as described in Material and Methods. Protein expression was induced in stably transfected cells by the addition of copper sulphate ($CuSO_4$) and the amount of protein secreted into the cell culture supernatant was determined by quantitative four-layer ELISA (Material and Methods).

To optimize induction and protein expression different $CuSO_4$ concentrations were compared and the course of protein expression was monitored for nine days. Protein secreted into cell culture supernatant was quantified by four-layer ELISA (Material and Methods). As an example, the expression of sEH1H2 $_{444}$ is shown in figure 19. The highest expression levels were observed after induction with 1mM and 1.25mM $CuSO_4$ at day nine. Cell density reached approximately $2x10^7$ cells/ml after 7-10 days of induction. Since 1.25mM $CuSO_4$ occasionally caused decreased cell growth and cell death, 1mM $CuSO_4$ was used for all experiments. At the time point of harvest the pH of the cell culture supernatant was in the range of 6.1 to 6.5.

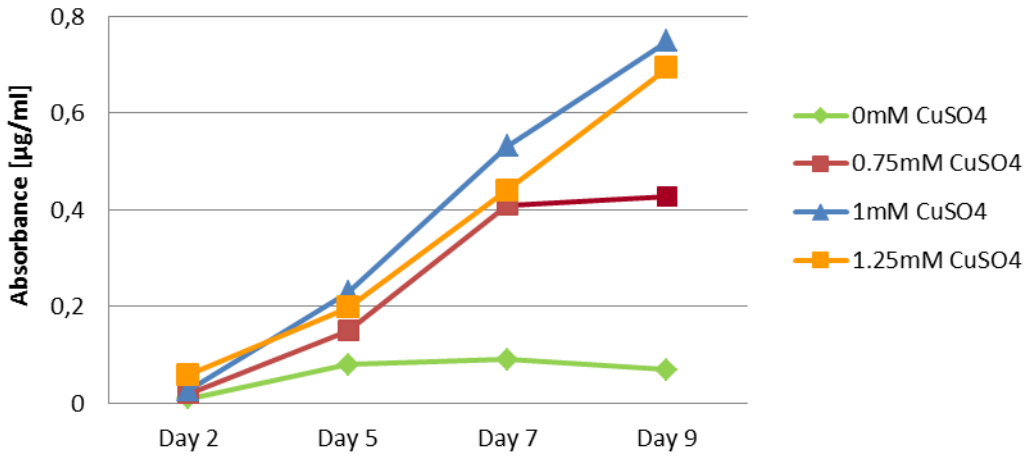

Figure 19 Time course of sEH1H2 $_{444}$ secretion into the cell culture supernatant of stably transfected S2 cells as quantified by a four-layer ELISA. Days after induction with different $CuSO_4$ concentrations are depicted on the abscissa.

5.2.3 Small scale purification of sEH1H2 $_{444\ dstrep}$

In order to express sEH1H2 $_{444\ dstrep}$, the respective stably transfected S2 cells, were induced with 1mM of $CuSO_4$ in serum free medium. Cell culture supernatant was harvested at a cell density of 1-2x10^7 cells/ml at day nine, was clarified and concentrated by ultrafiltration (Material and Methods). sEH1H2 $_{444\ dstrep}$ was purified in small scale by affinity chromatography, making use of the binding of strep tag II to the streptactin resin. The purification was carried out as described in Material and Methods. Briefly, the concentrated cell culture supernatant was applied to equilibrated streptactin spin columns. Bound protein was eluted with 2mM D-Biotin. The concentration of the E protein was determined in a quantitative four-layer ELISA. As shown in figure 20 and reminiscent of sEH1H2 $_{448\ dstrep}$ (unpublished data), about 80% of the protein did not bind to the streptactin spin column and only 2% of the attached material could be eluted with D-Biotin (Figure 20).

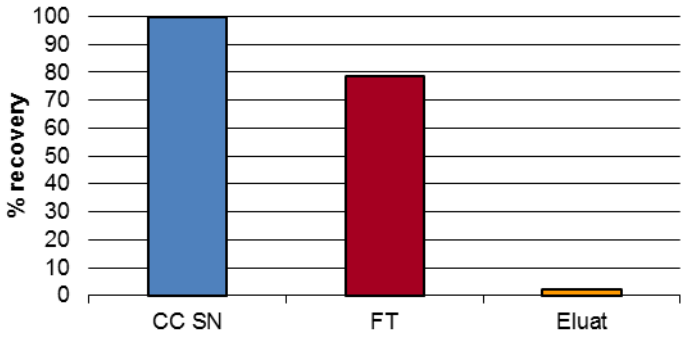

Figure 20 Recovery diagram of purification of sEH1H2 $_{444\ dstrep}$ with a streptactin spin column as measured by a quantitative four-layer ELISA. Amount of E protein in the original cell culture supernatant (*CC SN*) was defined as 100%.
FT: Flow through the affinity column
Eluat: Bound protein eluted by D-Biotin from the affinity column

5.2.4 Prevention of aggregation of sEH1H2 proteins

To test the hypothesis whether sEH1H2 $_{448}$ and sEH1H2 $_{444}$ form aggregates in the cell culture supernatant (that are unable to bind to streptactin columns), solubilization experiments with different detergent, were carried out. For this purpose, cell culture supernatant containing sEH1H2 $_{448}$ was solubilized with CHAPS, n-Octyl-ß-D-glycopyranoside (n-OG), n-Dodecyl-ß-D-maltoside (DDM) or Triton X-100 (TX-100). CHAPS, a zwitterionic detergent, is not suitable for crystallization, but can be easily removed prior to crystallization, because of its low micelle molecular weight (6.2 kDa). The other three detergents are non-ionic, with n-OG and DDM being suitable for crystallization. In contrast TX-100, is not recommended for crystallization (Prive, 2007) and its removal is difficult due to its high micelle molecular weight (88 kDa). TX-100, however, was included as a control, because of its previous use in the solubilization of full-length E trimers (Allison et al., 1995a; Stiasny et al., 2005). Cell culture supernatant samples of 800µl were incubated for one hour at room temperature with 200µl of the respective detergent and then centrifuged for 30 minutes at 4°C at 14,000 rpm (Eppendorf, 5417R). The supernatants were collected and pellets were resuspended in the previous volume with TAN buffer pH=8.0 with 0.5 % TX-100. The amount of E protein in both fractions was determined by a

quantitative four-layer ELISA (Figure 21).

Solubility of sEH1H2 $_{448}$ could be increased with all four detergents compared to the control without detergent in which 42% of the material was found in the pellet (Figure 21). After incubation with TX-100 or DDM about 98% of the protein was found in the supernatant, while in the presence of n-OG 95% of the protein was found in the supernatant (Figure 21). With CHAPS 75% of the protein was detected in the supernatant (Figure 21).

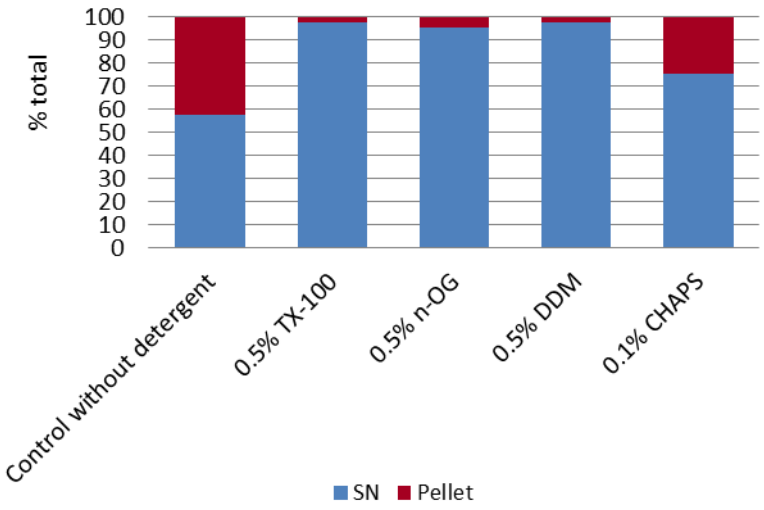

Figure 21 Recovery diagram of solubilization and low-speed centrifugation of sEH1H2 containing cell culture SN using different detergents. sEH1H2 $_{448}$ concentration after centrifugation was determined in supernatant and pellet by a quantitative four-layer ELISA.

5.2.5 Purification of sEH1H2 $_{448}$ without tag

Since tag-less proteins containing the whole stem region would be preferred for crystallization trials, it was attempted to purify the protein via ion-exchange chromatography similar to the method described by Nayak et al. (Nayak et al., 2009). For this purpose, Schneider S2 cells stably transfected with the sEH1H2 $_{448}$ plasmid were adapted to serum free medium and scaled up to 500ml (Material and Methods). After induction of expression, cells were propagated for nine days, harvested, solubilized with N-Dodecyl ß-D-maltoside (DDM), and clarified. After a buffer exchange into 20mM MES (pH=6.1) containing DDM, sEH1H2 $_{448}$ was subjected to cation-exchange chromatography using HITRAP SP FF columns as described in

Material and Methods. The amount of E protein in the collected fractions was quantified by a four-layer ELISA (Material and Methods). As shown in figure 22 A and figure 22 B, the peak containing E protein represented about 40% of the input material. In the FPLC UV absorbance profile (Figure 22 C), a broad peak was observed with a small shoulder at the position of $sEH1H2_{448}$ indicating a low purity of the $sEH1H2_{448}$ protein which was confirmed by SDS-PAGE (Figure 23). Further optimization experiments and additional purification steps or alternative purification strategies are required for this protein.

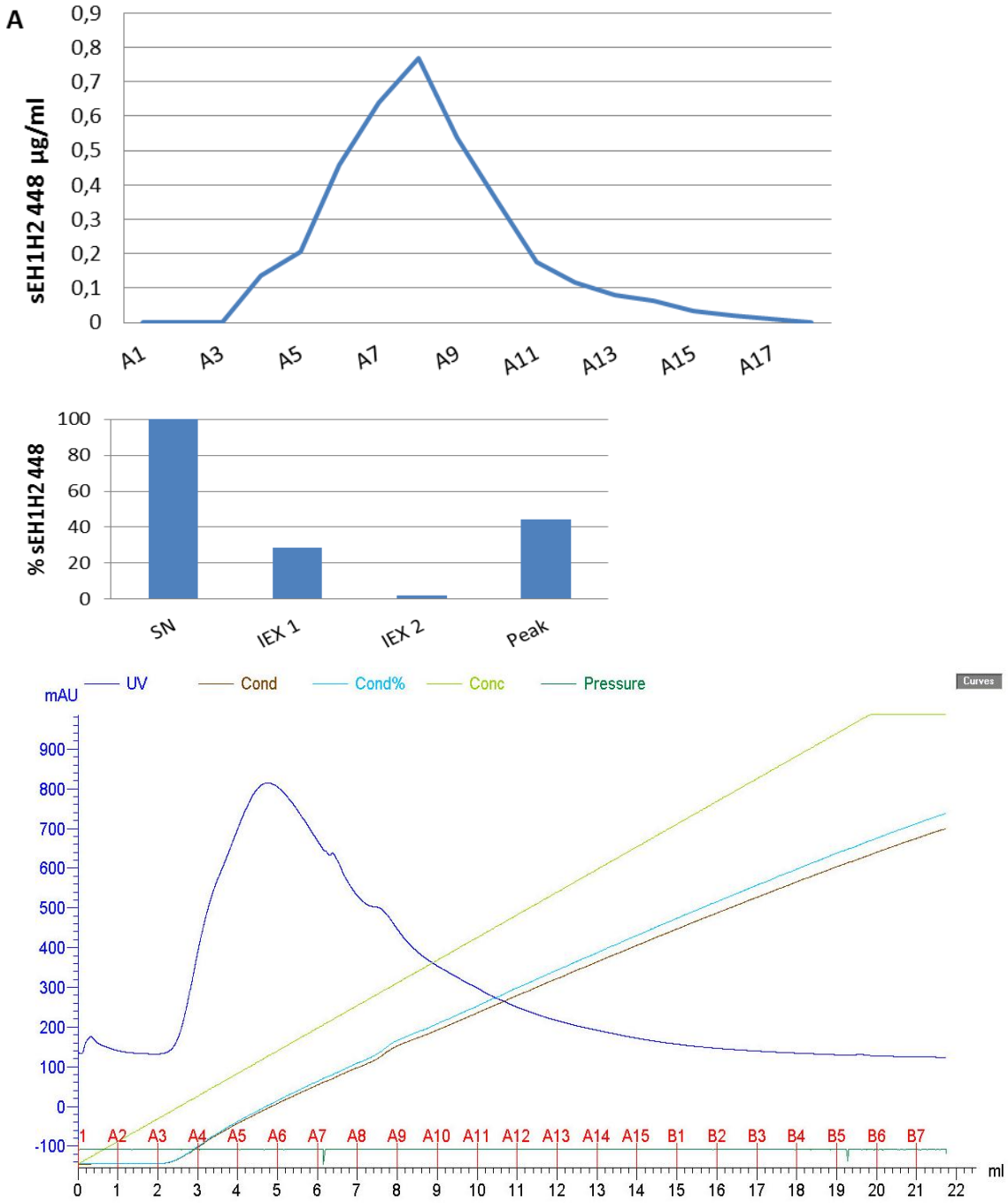

Figure 22 (A) sEH1H2 $_{448}$ in the FPLC fractions quantified by a four-layer ELISA. **(B)** Recovery diagram of sEH1H2 $_{448}$ purification by cation exchange chromatography. **(C)** Elution profile of cation exchange chromatography. Protein UV absorbance (mAU) in blue.

SN: applied cell culture supernatant

IEX 1: IEX flow through 1

IEX 2 : IEX flow through 2

Peak: pooled peak fractions

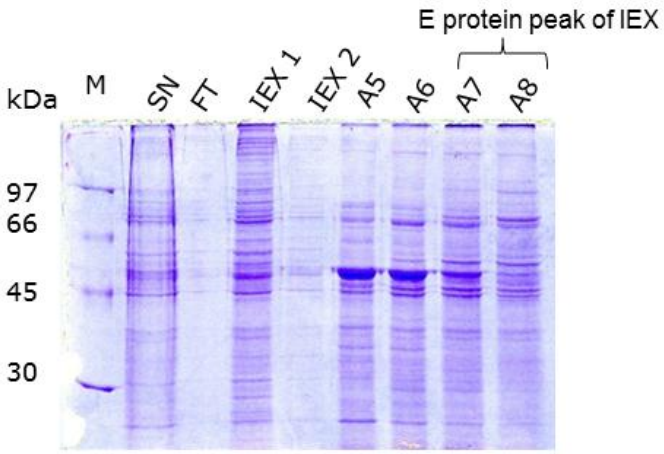

Figure 23 Coomassie stained SDS-PAGE. Samples of purification steps of sEH1H2 $_{448}$. Peak fractions five to eight (A5-A8). A7 and A8 are the peak of E protein after IEX chromatography.

SN: applied cell culture supernatant

FT: Buffer exchange flow through

IEX 1: IEX flow through 1

IEX 2 : IEX flow through 2

5.3 Characterization of sEH1H2

5.3.1 Oligomeric state of sEH1H2

To investigate the oligomeric structure of sEH1H2 $_{444/448,}$ a sedimentation analysis was carried out as described previously (Stiasny et al., 2004; Stiasny et al., 2005). Solubilized and concentrated cell culture supernatant of sEH1H2 $_{444}$ and sEH1H2 $_{448}$ were subjected to sedimentation in 7-20% (wt/wt) continuous sucrose gradients that allow a separation of dimers and trimers. Solubilized low pH treated (trimer) and untreated (dimer) virus were used as controls. As shown in figure 24 A, about 59% of sEH1H2 $_{444}$ was found in fractions corresponding to dimers and approximately 39% in fractions corresponding to trimers. sEH1H2 $_{448}$ mainly sedimented in trimer fractions (~71%) (Figure 24 B).

To confirm the oligomeric state of the protein, the peak fractions were chemically cross-linked with DMS as described in Material and Methods. In the case

of sEH1H2 $_{448}$, a trimeric band was clearly visible, thus confirming the results of the sedimentation analysis. The concentration of sEH1H2 $_{444}$ in the peak fractions was too low for cross-linking.

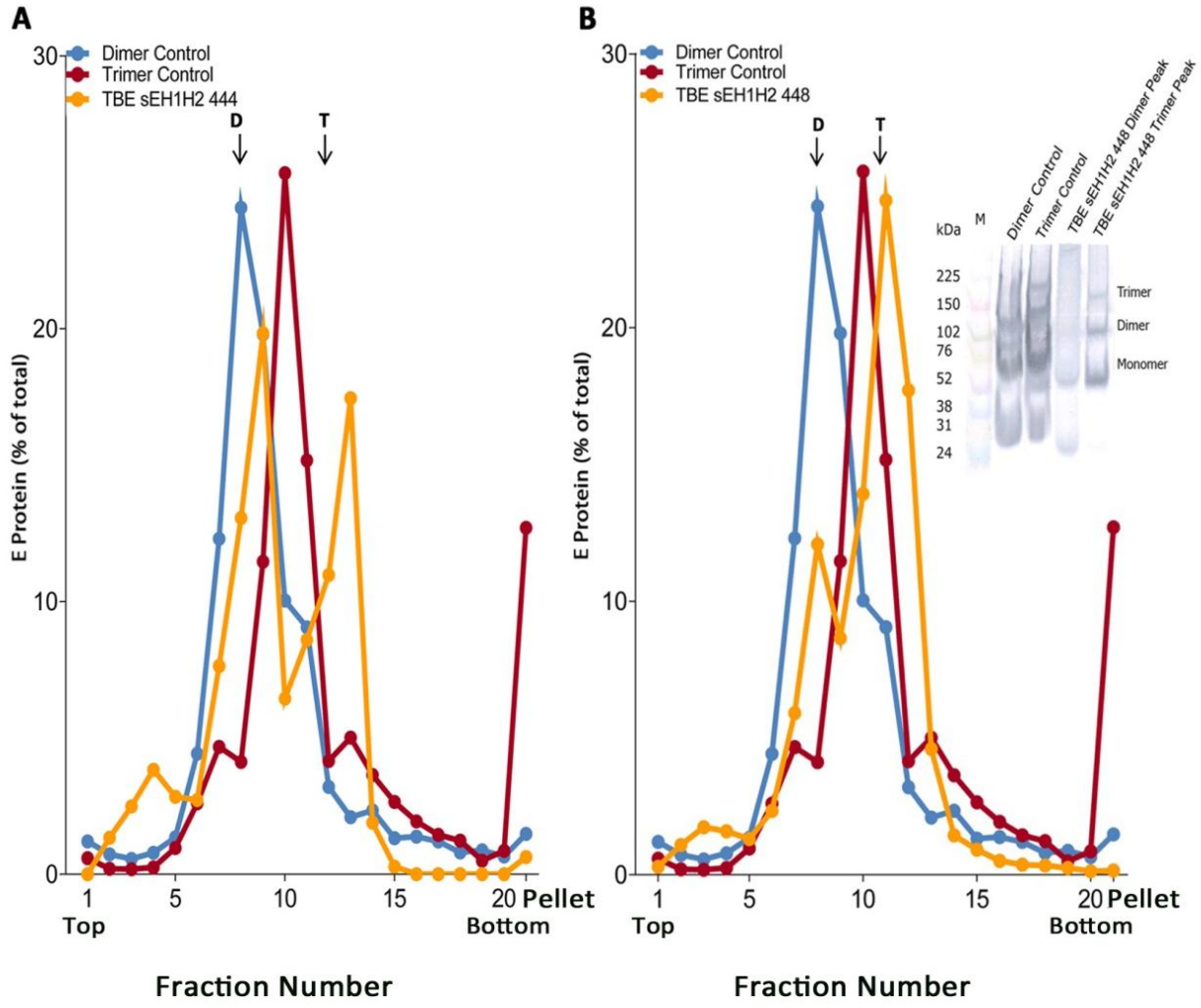

Figure 24 Sedimentation analysis of **(A)** sEH1H2 $_{444}$ and **(B)** sEH1H2 $_{448}$ in the presence of detergent. The sedimentation direction is from left to right, the position of dimers (D) and trimers (T) are indicated. Inset: Crosslinking of proteins in the peak fractions analyzed on a Western blot.

5.3.2 Reactivity of sE trimers with monoclonal antibodies

Since it has been speculated that the stem helix 2 could interact with the fusion peptide (FP) (Modis et al., 2004), we probed its accessibility in ELISA with an FP-specific mab and trimers with different carboxy-termini. These trimers included the truncated sE without the whole stem-anchor region (sE trimer (Stiasny et al., 2004)), the truncated sE trimer containing helix 1 of the stem (sEH1 trimer), the truncated sE trimer containing the whole stem region (sEH1 448 trimer) and the full-length E trimer isolated from solubilized virions (E trimer). The different trimer preparations were captured either with the FP specific mab 4G2 (Stiasny et al., 2006) or the DIII specific mab B2 (Kiermayr et al., 2009) (Figure 25). The bound trimers were detected with polyclonal rabbit anti-TBEV serum (Material and Methods). As shown in figure 26, the FP was fully accessible in the trimers lacking helix 2, whereas the reactivity of 4G2 was strongly reduced in the trimers containing helix 2. Interestingly, there was no difference in the reactivity of 4G2 with the sEH1H2 trimer and the full length E trimer indicating that the shielding of the fusion peptide occurs mainly by helix 2 and not the transmembrane domains.

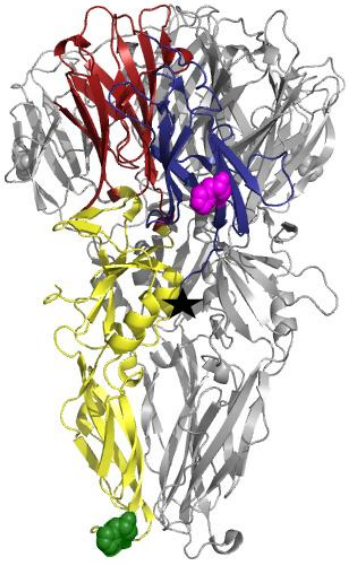

Figure 25 Ribbon diagram of the TBEV sE trimer. The balls indicate the position of mutations that affected binding of mabs (magenta: B2, green: 4G2). The black star indicates the C-terminus where the stem starts. The figure was generated with PyMOL Molecular Graphics System, Version 1.3, Schrödinger, LLC.

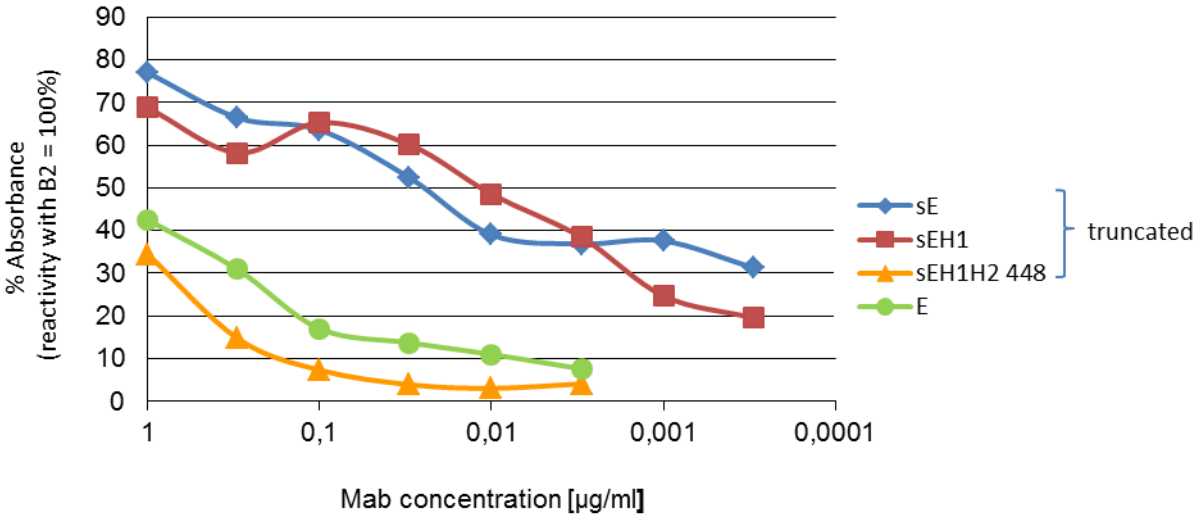

Figure 26 Four-layer ELISA with different trimers and mabs. Absorbance values of 4G2 are expressed as percentage of B2 absorbance values.

sE: sE trimers missing the whole stem-anchor region

sEH1: sE trimers including helix 1

sEH1H2 $_{448}$: sE trimers including the stem region until amino acid 448

E: full length E trimers from solubilized virions

6 Discussion

The atomic structures of the postfusion sE trimers lack the important stem-anchor region. Fusion models suggest that the stem zippers along the body of the trimer during the low-pH-induced conformational changes of E thereby leading to the formation of the stable postfusion trimer and providing part of the energy required for fusion (Harrison, 2008; Stiasny and Heinz, 2006). This hypothesis is supported by modeling studies with helix 1of the stem (Bressanelli et al., 2004) and a mutagenesis study with TBEV RSPs that identified a stem domain II interaction site (Pangerl et al., 2011).

In the course of this diploma thesis, recombinant postfusion trimers of TBEV containing the stem helix 1 (sEH1) and the whole stem region (sEH1H2 $_{448}$) were generated to shed light on the precise role of the stem in fusion. The proteins were produced in the *Drosophila* expression system. Similar to the recombinant sE proteins of dengue virus types2 and 3 lacking the whole stem-anchor region (Modis et al., 2003; Modis et al., 2005; Zhang et al., 2004), sEH1 was predominantly secreted as a dimer into the cell culture supernatant and could be converted into trimers by acidification in presence of liposomes as described previously (Modis et al., 2004; Stiasny et al., 2004). In contrast, the cell culture supernatant of stably transfected sEH1H2 $_{448}$ *Drosophila* S2 cells contained about 80% trimers. Removal of four carboxy-terminal amino acids of sEH1H2 decreased strongly the efficiency of trimerization (sEH1H2 $_{444}$) indicating that the complete stem helix 2 acts as a “faciliator” for trimerization. However, it is not clear from our data whether trimerization already occurred in the cell or in the slightly acidic culture supernatant of S2 cells.

The trimeric structure of sEH1H2 $_{448}$ probably caused the difficulties observed in the attempts to purify the protein. As shown previously, sE trimers lacking the whole stem-anchor region were already more hydrophobic than monomers and dimers (Stiasny et al., 2004) and the presence of the stem helix 2 further increased the hydrophobicity of the protein. This presumably led to the strong aggregation of sEH1H2 in the cell culture supernatant and purification procedures will require the use of detergents.

An involvement of pre-transmembrane elements (membrane proximal external

regions; MPERs) in fusion was shown for other viral fusion proteins (reviewed in (Lorizate et al., 2008)). It has been suggested that the MPERs either transmit protein conformational energy into membranes and/or perturb lipid bilayers integrity thus facilitating fusion (Lorizate et al., 2008). The stem helix 2 of dengue virus was also shown to be able to bind to lipid membranes in an *in vitro* experiment using a recombinant form of helix 2 (Lin et al., 2011). It is thus possible that helix 2 acts in a similar fashion as the MPERs of other fusion proteins. In this context, it is important to note that stem helix 2 peptides of dengue virus were shown to bind to virions at neutral pH, presumably by interacting with the viral membrane, and block low-pH-induced fusion (Schmidt et al., 2010a; Schmidt et al., 2010b). It has been suggested that these peptides interact with an E intermediate generated during the conformational changes of E necessary for fusion (Schmidt et al., 2010a; Schmidt et al., 2010b).

Although, purified sEH1H2 $_{448}$ proteins were not obtained during this thesis, preliminary studies using sEH1H2 containing cell culture supernatant and monoclonal antibodies allowed a comparison with different trimeric forms of E. These included truncated sE trimers lacking the whole stem-anchor region (Stiasny et al., 2004), sEH1 containing the first stem helix (this thesis) and full-length E trimers isolated from low-pH-treated and solubilized virions (Stiasny et al., 2005). The results obtained indicate that helix 2 interacts with the FP at the tip of domain II in the postfusion trimer, because an FP specific mab exhibited a similar reduced reactivity with full-length and sEH1H2 trimers compared to trimers without helix 2. The stem might therefore follow the groove formed by neighboring DIIs with helix 2 extending to the FPs, as speculated after elucidation of the atomic structure of sE trimers lacking the whole stem-anchor region (Bressanelli et al., 2004; Modis et al., 2004). The FPs interact with each other in these truncated sE trimers and it is possible that in the full-length trimer the stem keeps the FPs apart, similar to the structurally closely related postfusion E1 trimer of alphaviruses (Bressanelli et al., 2004; Gibbons et al., 2004b). It has been proposed that the more “open conformation” of truncated E1 is due to the fact that the stem of this fragment extends further towards the FPs than in the case of the flavivirus sE (Bressanelli et al., 2004).

To determine whether the stem might push the FPs apart and to define the precise interactions of the stem with the FPs and other parts of domain II, high

resolution X-ray structures of sE trimers containing the stem are necessary. We were able to produce recombinant sEH1 trimers in sufficient amounts and quality for crystallization trials, but for the isolation and purification of sEH1H2 trimers further optimization experiments are required.

7 References

Allison, S.L., J. Schalich, K. Stiasny, C.W. Mandl, and F.X. Heinz. 2001. Mutational evidence for an internal fusion peptide in flavivirus envelope protein E. *J Virol*. 75:4268-4275.

Allison, S.L., J. Schalich, K. Stiasny, C.W. Mandl, C. Kunz, and F.X. Heinz. 1995a. Oligomeric rearrangement of tick-borne encephalitis virus envelope proteins induced by an acidic pH. *J Virol*. 69:695-700.

Allison, S.L., K. Stadler, C.W. Mandl, C. Kunz, and F.X. Heinz. 1995b. Synthesis and secretion of recombinant tick-borne encephalitis virus protein E in soluble and particulate form. *J Virol*. 69:5816-5820.

Altmann, F., E. Staudacher, I.B. Wilson, and L. Marz. 1999. Insect cells as hosts for the expression of recombinant glycoproteins. *Glycoconj J*. 16:109-123.

Backovic, M., and T.S. Jardetzky. 2009. Class III viral membrane fusion proteins. *Curr Opin Struct Biol*. 19:189-196.

Bressanelli, S., K. Stiasny, S.L. Allison, E.A. Stura, S. Duquerroy, J. Lescar, F.X. Heinz, and F.A. Rey. 2004. Structure of a flavivirus envelope glycoprotein in its low-pH-induced membrane fusion conformation. *EMBO J*. 23:728-738.

Bunch, T.A., Y. Grinblat, and L.S. Goldstein. 1988. Characterization and use of the Drosophila metallothionein promoter in cultured Drosophila melanogaster cells. *Nucleic Acids Res*. 16:1043-1061.

Chambers, T.J., C.S. Hahn, R. Galler, and C.M. Rice. 1990. Flavivirus genome organization, expression, and replication. *Annu Rev Microbiol*. 44:649-688.

Crill, W.D., H.R. Hughes, M.J. Delorey, and G.J. Chang. 2009. Humoral immune responses of dengue fever patients using epitope-specific serotype-2 virus-like particle antigens. *PLoS One*. 4:e4991.

Demain, A.L., and P. Vaishnav. 2009. Production of recombinant proteins by microbes and higher organisms. *Biotechnol Adv*. 27:297-306.

Drummond AJ, A.B., Buxton S, Cheung M, Cooper A, Duran C, Field M, Heled J, Kearse M, Markowitz S, Moir R, Stones-Havas S, Sturrock S, Thierer T, Wilson A. 2011. Geneious v5.4. http://www.geneious.com/.

Ecker, M., S.L. Allison, T. Meixner, and F.X. Heinz. 1999. Sequence analysis and genetic classification of tick-borne encephalitis viruses from Europe and Asia. *J Gen Virol*. 80 (Pt 1):179-185.

Fritz, R., K. Stiasny, and F.X. Heinz. 2008. Identification of specific histidines as pH sensors in flavivirus membrane fusion. *J Cell Biol*. 183:353-361.

Geller, B. 2009. Expression of Recombinant Flavivirus E Proteins. Uiversity of Vienna, Vienna.

Gibbons, D.L., B. Reilly, A. Ahn, M.C. Vaney, A. Vigouroux, F.A. Rey, and M. Kielian. 2004a. Purification and crystallization reveal two types of interactions of the fusion protein homotrimer of Semliki Forest virus. *J Virol*. 78:3514-3523.

Gibbons, D.L., M.C. Vaney, A. Roussel, A. Vigouroux, B. Reilly, J. Lepault, M. Kielian, and F.A. Rey. 2004b. Conformational change and protein-protein interactions of the fusion protein of Semliki Forest virus. *Nature*. 427:320-325.

Gubler, D.J., Kuno G., Markoff L. 2007. Flaviviruses. *In* Fields Virology, 5th ed. Lippincott Williams & Wilkins Co., Philadelphia, PA.

. D.M.H. Knipe, P.M., editor, Philadelphia. 1153-1252.

Hacker, K., L. White, and A.M. de Silva. 2009. N-linked glycans on dengue viruses grown in mammalian and insect cells. *J Gen Virol*. 90:2097-2106.

Harrison, S.C. 2005. Mechanism of membrane fusion by viral envelope proteins. *Adv Virus Res*. 64:231-261.

Harrison, S.C. 2008. Viral membrane fusion. *Nat Struct Mol Biol*. 15:690-698.

Heinz, F., and C. Kunz. 1977. Characterization of tick-borne encephalitis virus and immunogenicity of its surface components in mice. *Acta Virol*. 21:308-316.

Heinz, F.X., S.L. Allison, K. Stiasny, J. Schalich, H. Holzmann, C.W. Mandl, and C. Kunz. 1995. Recombinant and virion-derived soluble and particulate immunogens for vaccination against tick-borne encephalitis. *Vaccine*. 13:1636-1642.

Heinz, F.X., K. Stiasny, G. Puschner-Auer, H. Holzmann, S.L. Allison, C.W. Mandl, and C. Kunz. 1994. Structural changes and functional control of the tick-borne encephalitis virus glycoprotein E by the heterodimeric association with protein prM. *Virology*. 198:109-117.

Holzmann, H., S.W. Aberle, K. Stiasny, P. Werner, A. Mischak, B. Zainer, M. Netzer, S. Koppi, E. Bechter, and F.X. Heinz. 2009. Tick-borne encephalitis from eating goat cheese in a mountain region of Austria. *Emerg Infect Dis*. 15:1671-1673.

Jaiswal, S., N. Khanna, and S. Swaminathan. 2004. High-level expression and one-step purification of recombinant dengue virus type 2 envelope domain III protein in Escherichia coli. *Protein Expr Purif*. 33:80-91.

Jose, J., J.E. Snyder, and R.J. Kuhn. 2009. A structural and functional perspective of alphavirus replication and assembly. *Future Microbiol*. 4:837-856.

Kanai, R., K. Kar, K. Anthony, L.H. Gould, M. Ledizet, E. Fikrig, W.A. Marasco, R.A. Koski, and Y. Modis. 2006. Crystal structure of west nile virus envelope glycoprotein reveals viral surface epitopes. *J Virol*. 80:11000-11008.

Kaufmann, B., P.R. Chipman, H.A. Holdaway, S. Johnson, D.H. Fremont, R.J. Kuhn, M.S. Diamond, and M.G. Rossmann. 2009. Capturing a flavivirus pre-fusion intermediate. *PLoS Pathog*. 5:e1000672.

Kaufmann, B., and M.G. Rossmann. 2011. Molecular mechanisms involved in the early steps of flavivirus cell entry. *Microbes Infect*. 13:1-9.

Kielian, M. 2006. Class II virus membrane fusion proteins. *Virology*. 344:38-47.

Kielian, M., and F.A. Rey. 2006. Virus membrane-fusion proteins: more than one way to make a hairpin. *Nat Rev Microbiol*. 4:67-76.

Kiermayr, S., K. Stiasny, and F.X. Heinz. 2009. Impact of quaternary organization on the antigenic structure of the tick-borne encephalitis virus envelope glycoprotein E. *J Virol*. 83:8482-8491.

Kim, Y.K., H.S. Shin, N. Tomiya, Y.C. Lee, M.J. Betenbaugh, and H.J. Cha. 2005. Production and N-glycan analysis of secreted human erythropoietin glycoprotein in stably transfected Drosophila S2 cells. *Biotechnol Bioeng*. 92:452-461.

Kojima, A., A. Yasuda, H. Asanuma, T. Ishikawa, A. Takamizawa, K. Yasui, and T. Kurata. 2003. Stable high-producer cell clone expressing virus-like particles of the Japanese encephalitis virus e protein for a second-generation subunit vaccine. *J Virol*. 77:8745-8755.

Konishi, E., S. Pincus, E. Paoletti, R.E. Shope, T. Burrage, and P.W. Mason. 1992. Mice immunized with a subviral particle containing the Japanese encephalitis virus prM/M and E proteins are protected from lethal JEV infection. *Virology*. 188:714-720.

Kuhn, R.J., W. Zhang, M.G. Rossmann, S.V. Pletnev, J. Corver, E. Lenches, C.T. Jones, S. Mukhopadhyay, P.R. Chipman, E.G. Strauss, T.S. Baker, and J.H. Strauss. 2002. Structure of dengue virus: implications for flavivirus organization, maturation, and fusion. *Cell*. 108:717-725.

Kuno, G., G.J. Chang, K.R. Tsuchiya, N. Karabatsos, and C.B. Cropp. 1998. Phylogeny of the genus Flavivirus. *J Virol*. 72:73-83.

Lescar, J., A. Roussel, M.W. Wien, J. Navaza, S.D. Fuller, G. Wengler, and F.A. Rey. 2001. The Fusion glycoprotein shell of Semliki Forest virus: an icosahedral assembly primed for fusogenic activation at endosomal pH. *Cell*. 105:137-148.

Li, L., S.M. Lok, I.M. Yu, Y. Zhang, R.J. Kuhn, J. Chen, and M.G. Rossmann. 2008. The flavivirus precursor membrane-envelope protein complex: structure and maturation. *Science*. 319:1830-1834.

Liao, M., and M. Kielian. 2006a. Functions of the stem region of the Semliki Forest virus fusion protein during virus fusion and assembly. *J Virol*. 80:11362-11369.

Liao, M., and M. Kielian. 2006b. Site-directed antibodies against the stem

region reveal low pH-induced conformational changes of the Semliki Forest virus fusion protein. *J Virol*. 80:9599-9607.

Lieberman, M.M., D.E. Clements, S. Ogata, G. Wang, G. Corpuz, T. Wong, T. Martyak, L. Gilson, B.A. Coller, J. Leung, D.M. Watts, R.B. Tesh, M. Siirin, A. Travassos da Rosa, T. Humphreys, and C. Weeks-Levy. 2007. Preparation and immunogenic properties of a recombinant West Nile subunit vaccine. *Vaccine*. 25:414-423.

Lin, S.R., G. Zou, S.C. Hsieh, M. Qing, W.Y. Tsai, P.Y. Shi, and W.K. Wang. 2011. The helical domains of the stem region of dengue virus envelope protein are involved in both virus assembly and entry. *J Virol*. 85:5159-5171.

Lindenbach B.D. Thiel H-J., R.C.M. 2007. Fields Virology. *In* Flaviviridae: The Viruses and Their Replication H.P.M. Knipe D.M., editor. Lippincott-Raven Publishers, Philadelphia. 1101-1113.

Lindquist, L., and O. Vapalahti. 2008. Tick-borne encephalitis. *Lancet*. 371:1861-1871.

Liu, W., H. Jiang, J. Zhou, X. Yang, Y. Tang, D. Fang, and L. Jiang. 2010. Recombinant dengue virus-like particles from Pichia pastoris: efficient production and immunological properties. *Virus Genes*. 40:53-59.

Lorenz, I.C., S.L. Allison, F.X. Heinz, and A. Helenius. 2002. Folding and dimerization of tick-borne encephalitis virus envelope proteins prM and E in the endoplasmic reticulum. *J Virol*. 76:5480-5491.

Lorizate, M., N. Huarte, A. Saez-Cirion, and J.L. Nieva. 2008. Interfacial pre-transmembrane domains in viral proteins promoting membrane fusion and fission. *Biochim Biophys Acta*. 1778:1624-1639.

Luca, V.C., J. Abimansour, C.A. Nelson, and D.H. Fremont. 2011. Crystal structure of the Japanese encephalitis virus envelope protein. *J Virol*.

Mandl, C.W., F.X. Heinz, and C. Kunz. 1988. Sequence of the structural proteins of tick-borne encephalitis virus (western subtype) and comparative analysis with other flaviviruses. *Virology*. 166:197-205.

Maroni, G., D. Lastowski-Perry, E. Otto, and D. Watson. 1986. Effects of heavy metals on Drosophila larvae and a metallothionein cDNA. *Environ Health Perspect*. 65:107-116.

Mason, P.W., S. Pincus, M.J. Fournier, T.L. Mason, R.E. Shope, and E. Paoletti. 1991. Japanese encephalitis virus-vaccinia recombinants produce particulate forms of the structural membrane proteins and induce high levels of protection against lethal JEV infection. *Virology*. 180:294-305.

Modis, Y., S. Ogata, D. Clements, and S.C. Harrison. 2003. A ligand-binding pocket in the dengue virus envelope glycoprotein. *Proc Natl Acad Sci U S A*. 100:6986-6991.

Modis, Y., S. Ogata, D. Clements, and S.C. Harrison. 2004. Structure of the dengue virus envelope protein after membrane fusion. *Nature*. 427:313-319.

Modis, Y., S. Ogata, D. Clements, and S.C. Harrison. 2005. Variable surface epitopes in the crystal structure of dengue virus type 3 envelope glycoprotein. *J Virol*. 79:1223-1231.

Mukhopadhyay, S., B.S. Kim, P.R. Chipman, M.G. Rossmann, and R.J. Kuhn. 2003. Structure of West Nile virus. *Science*. 302:248.

Mukhopadhyay, S., R.J. Kuhn, and M.G. Rossmann. 2005. A structural perspective of the flavivirus life cycle. *Nat Rev Microbiol*. 3:13-22.

Mukhopadhyay, S., W. Zhang, S. Gabler, P.R. Chipman, E.G. Strauss, J.H. Strauss, T.S. Baker, R.J. Kuhn, and M.G. Rossmann. 2006. Mapping the structure and function of the E1 and E2 glycoproteins in alphaviruses. *Structure*. 14:63-73.

Nayak, V., M. Dessau, K. Kucera, K. Anthony, M. Ledizet, and Y. Modis. 2009. Crystal structure of dengue virus type 1 envelope protein in the postfusion conformation and its implications for membrane fusion. *J Virol*. 83:4338-4344.

Nowak, T., P.M. Farber, and G. Wengler. 1989. Analyses of the terminal sequences of West Nile virus structural proteins and of the in vitro translation of these proteins allow the proposal of a complete scheme of the proteolytic cleavages involved in their synthesis. *Virology*. 169:365-376.

Nybakken, G.E., C.A. Nelson, B.R. Chen, M.S. Diamond, and D.H. Fremont. 2006. Crystal structure of the West Nile virus envelope glycoprotein. *J Virol*. 80:11467-11474.

Ohtaki, N., H. Takahashi, K. Kaneko, Y. Gomi, T. Ishikawa, Y. Higashi, T. Kurata, T. Sata, and A. Kojima. 2010. Immunogenicity and efficacy of two types of West Nile virus-like particles different in size and maturation as a second-generation vaccine candidate. *Vaccine*. 28:6588-6596.

Pangerl, K., F.X. Heinz, and K. Stiasny. 2011. Mutational analysis of the zippering reaction during flavivirus membrane fusion. *J Virol*.

Prive, G.G. 2007. Detergents for the stabilization and crystallization of membrane proteins. *Methods*. 41:388-397.

Rey, F.A., F.X. Heinz, C. Mandl, C. Kunz, and S.C. Harrison. 1995. The envelope glycoprotein from tick-borne encephalitis virus at 2 A resolution. *Nature*. 375:291-298.

Sanchez-San Martin, C., C.Y. Liu, and M. Kielian. 2009. Dealing with low pH: entry and exit of alphaviruses and flaviviruses. *Trends Microbiol*. 17:514-521.

Schalich, J., S.L. Allison, K. Stiasny, C.W. Mandl, C. Kunz, and F.X. Heinz. 1996. Recombinant subviral particles from tick-borne encephalitis virus are fusogenic and provide a model system for studying flavivirus envelope glycoprotein functions. *J*

Virol. 70:4549-4557.

Schibli, D.J., and W. Weissenhorn. 2004. Class I and class II viral fusion protein structures reveal similar principles in membrane fusion. *Mol Membr Biol*. 21:361-371.

Schmidt, A.G., P.L. Yang, and S.C. Harrison. 2010a. Peptide inhibitors of dengue-virus entry target a late-stage fusion intermediate. *PLoS Pathog*. 6:e1000851.

Schmidt, A.G., P.L. Yang, and S.C. Harrison. 2010b. Peptide Inhibitors of Flavivirus Entry Derived from the E-protein Stem. *J Virol*.

Skehel, J.J., and D.C. Wiley. 1998. Coiled coils in both intracellular vesicle and viral membrane fusion. *Cell*. 95:871-874.

Skehel, J.J., and D.C. Wiley. 2000. Receptor binding and membrane fusion in virus entry: the influenza hemagglutinin. *Annu Rev Biochem*. 69:531-569.

Stiasny, K., S.L. Allison, A. Marchler-Bauer, C. Kunz, and F.X. Heinz. 1996. Structural requirements for low-pH-induced rearrangements in the envelope glycoprotein of tick-borne encephalitis virus. *J Virol*. 70:8142-8147.

Stiasny, K., S.L. Allison, J. Schalich, and F.X. Heinz. 2002. Membrane interactions of the tick-borne encephalitis virus fusion protein E at low pH. *J Virol*. 76:3784-3790.

Stiasny, K., S. Bressanelli, J. Lepault, F.A. Rey, and F.X. Heinz. 2004. Characterization of a membrane-associated trimeric low-pH-induced Form of the class II viral fusion protein E from tick-borne encephalitis virus and its crystallization. *J Virol*. 78:3178-3183.

Stiasny, K., and F.X. Heinz. 2006. Flavivirus membrane fusion. *J Gen Virol*. 87:2755-2766.

Stiasny, K., S. Kiermayr, H. Holzmann, and F.X. Heinz. 2006. Cryptic properties of a cluster of dominant flavivirus cross-reactive antigenic sites. *J Virol*. 80:9557-9568.

Stiasny, K., C. Kossl, and F.X. Heinz. 2005. Differences in the postfusion conformations of full-length and truncated class II fusion protein E of tick-borne encephalitis virus. *J Virol*. 79:6511-6515.

Strauss, E.G., E.M. Lenches, and J.H. Strauss. 2002. Molecular genetic evidence that the hydrophobic anchors of glycoproteins E2 and E1 interact during assembly of alphaviruses. *J Virol*. 76:10188-10194.

Sugrue, R.J., T. Cui, Q. Xu, J. Fu, and Y.C. Chan. 1997a. The production of recombinant dengue virus E protein using Escherichia coli and Pichia pastoris. *J Virol Methods*. 69:159-169.

Sugrue, R.J., J. Fu, J. Howe, and Y.C. Chan. 1997b. Expression of the dengue

virus structural proteins in Pichia pastoris leads to the generation of virus-like particles. *J Gen Virol*. 78 (Pt 8):1861-1866.

Tripathi, N.K., J.P. Babu, A. Shrivastva, M. Parida, A.M. Jana, and P.V. Rao. 2008. Production and characterization of recombinant dengue virus type 4 envelope domain III protein. *J Biotechnol*. 134:278-286.

Umareddy, I., O. Pluquet, Q.Y. Wang, S.G. Vasudevan, E. Chevet, and F. Gu. 2007. Dengue virus serotype infection specifies the activation of the unfolded protein response. *Virol J*. 4:91.

van der Schaar, H.M., M.J. Rust, C. Chen, H. van der Ende-Metselaar, J. Wilschut, X. Zhuang, and J.M. Smit. 2008. Dissecting the cell entry pathway of dengue virus by single-particle tracking in living cells. *PLoS Pathog*. 4:e1000244.

Volk, D.E., D.W. Beasley, D.A. Kallick, M.R. Holbrook, A.D. Barrett, and D.G. Gorenstein. 2004. Solution structure and antibody binding studies of the envelope protein domain III from the New York strain of West Nile virus. *J Biol Chem*. 279:38755-38761.

Volk, D.E., L. Chavez, D.W. Beasley, A.D. Barrett, M.R. Holbrook, and D.G. Gorenstein. 2006. Structure of the envelope protein domain III of Omsk hemorrhagic fever virus. *Virology*. 351:188-195.

Volk, D.E., Y.C. Lee, X. Li, V. Thiviyanathan, G.D. Gromowski, L. Li, A.R. Lamb, D.W. Beasley, A.D. Barrett, and D.G. Gorenstein. 2007. Solution structure of the envelope protein domain III of dengue-4 virus. *Virology*. 364:147-154.

Volk, D.E., F.J. May, S.H. Gandham, A. Anderson, J.J. Von Lindern, D.W. Beasley, A.D. Barrett, and D.G. Gorenstein. 2009. Structure of yellow fever virus envelope protein domain III. *Virology*. 394:12-18.

von Bonsdorff, C.H., and S.C. Harrison. 1975. Sindbis virus glycoproteins form a regular icosahedral surface lattice. *J Virol*. 16:141-145.

Wang, P.G., M. Kudelko, J. Lo, L.Y. Siu, K.T. Kwok, M. Sachse, J.M. Nicholls, R. Bruzzone, R.M. Altmeyer, and B. Nal. 2009. Efficient assembly and secretion of recombinant subviral particles of the four dengue serotypes using native prM and E proteins. *PLoS One*. 4:e8325.

Weissenhorn, W., A. Hinz, and Y. Gaudin. 2007. Virus membrane fusion. *FEBS Lett*. 581:2150-2155.

White, J.M., S.E. Delos, M. Brecher, and K. Schornberg. 2008. Structures and mechanisms of viral membrane fusion proteins: multiple variations on a common theme. *Crit Rev Biochem Mol Biol*. 43:189-219.

Yu, I.M., H.A. Holdaway, P.R. Chipman, R.J. Kuhn, M.G. Rossmann, and J. Chen. 2009. Association of the pr peptides with dengue virus at acidic pH blocks membrane fusion. *J Virol*. 83:12101-12107.

Yu, I.M., W. Zhang, H.A. Holdaway, L. Li, V.A. Kostyuchenko, P.R. Chipman, R.J. Kuhn, M.G. Rossmann, and J. Chen. 2008. Structure of the immature dengue virus at low pH primes proteolytic maturation. *Science*. 319:1834-1837.

Zhang, W., P.R. Chipman, J. Corver, P.R. Johnson, Y. Zhang, S. Mukhopadhyay, T.S. Baker, J.H. Strauss, M.G. Rossmann, and R.J. Kuhn. 2003a. Visualization of membrane protein domains by cryo-electron microscopy of dengue virus. *Nat Struct Biol*. 10:907-912.

Zhang, Y., J. Corver, P.R. Chipman, W. Zhang, S.V. Pletnev, D. Sedlak, T.S. Baker, J.H. Strauss, R.J. Kuhn, and M.G. Rossmann. 2003b. Structures of immature flavivirus particles. *EMBO J*. 22:2604-2613.

Zhang, Y., W. Zhang, S. Ogata, D. Clements, J.H. Strauss, T.S. Baker, R.J. Kuhn, and M.G. Rossmann. 2004. Conformational changes of the flavivirus E glycoprotein. *Structure*. 12:1607-1618.

Zlatkovic, J., K. Stiasny, and F.X. Heinz. 2011. Immunodominance and functional activities of antibody responses to inactivated West Nile virus and recombinant subunit vaccines in mice. *J Virol*. 85:1994-2003.

Ich habe mich bemüht, sämtliche Inhaber der Bildrechte ausfindig zu machen und ihre Zustimmung zur Verwendung der Bilder in dieser Arbeit eingeholt. Sollte dennoch eine Urheberrechtsverletzung bekannt werden, ersuche ich um Meldung bei mir.

Curriculum Vitae

Andrea Bernhart

Persönliche Daten:

Geburtsdatum: 07.03.1987

Geburtsort: Wien, Österreich

Ausbildung:

1993-1997	Öffentliche Volksschule Knollgasse 4-6, 1170 Wien
1997-2005	Bundesgymnasium Maroltingergasse 69-71, 1160 Wien
2002	Academic semester as a student in EF Foundation for Forgein Study´s High School Year in New Zealand programme
2005	Matura mit ausgezeichnetem Erfolg
2005-2012	Studium der Molekularen Biologie an der Universität Wien
2010	(Februar-April) ERASMUS Praktikum bei Maria Angeles Muñoz Fernández, InmunoBiología Molecular, Hospital Gregorio Marañón, Madrid
2010-2012	Diplomarbeit am Department für Virologie